Journal for ImmunoTherapy of Cancer

Cell-free DNA copy number variations predict efficacy of immune checkpoint inhibitor-based therapy in hepatobiliary cancers

Xu Yang,[1] Ying Hu,[2] Keyan Yang,[3] Dongxu Wang,[1] Jianzhen Lin,[1] Junyu Long,[1] Fucun Xie,[1] Jinzhu Mao,[1] Jin Bian,[1] Mei Guan,[4] Jie Pan,[5] Li Huo,[6] Ke Hu,[7] Xiaobo Yang,[1] Yilei Mao,[1] Xinting Sang,[1] Jiao Zhang,[3] Xi Wang,[8] Henghui Zhang,[9,10] Haitao Zhao [1]

To cite: Yang X, Hu Y, Yang K, *et al*. Cell-free DNA copy number variations predict efficacy of immune checkpoint inhibitor-based therapy in hepatobiliary cancers. *Journal for ImmunoTherapy of Cancer* 2021;**9**:e001942. doi:10.1136/jitc-2020-001942

► Additional material is published online only. To view, please visit the journal online (http://dx.doi.org/10.1136/jitc-2020-001942).

XY, YH, KY and DW contributed equally.

XY, YH, KY and DW are joint first authors.

Accepted 22 February 2021

For numbered affiliations see end of article.

Correspondence to
Prof. Haitao Zhao;
zhaoht@pumch.cn

Prof. Henghui Zhang;
zhhbao@ccmu.edu.cn

Prof. Xi Wang;
xiwang@ccmu.edu.cn

ABSTRACT

Background This study was designed to screen potential biomarkers in plasma cell-free DNA (cfDNA) for predicting the clinical outcome of immune checkpoint inhibitor (ICI)-based therapy in advanced hepatobiliary cancers.

Methods Three cohorts including 187 patients with hepatobiliary cancers were recruited from clinical trials at the Peking Union Medical College Hospital. Forty-three patients received combination therapy of programmed cell death protein 1 (PD-1) inhibitor with lenvatinib (ICI cohort 1), 108 patients received ICI-based therapy (ICI cohort 2) and 36 patients received non-ICI therapy (non-ICI cohort). The plasma cfDNA and blood cell DNA mutation profiles were assessed to identify efficacy biomarkers by a cancer gene-targeted next-generation sequencing panel.

Results Based on the copy number variations (CNVs) in plasma cfDNA, the CNV risk score model was constructed to predict survival by using the least absolute shrinkage and selection operator Cox regression methods. The results of the two independent ICI-based therapy cohorts showed that patients with lower CNV risk scores had longer overall survival (OS) and progression-free survival (PFS) than those with high CNV risk scores (log-rank $p<0.01$). In the non-ICI cohort, the CNV risk score was not associated with PFS or OS. Furthermore, the results indicated that 53% of patients with low CNV risk scores achieved durable clinical benefit; in contrast, 88% of patients with high CNV risk scores could not benefit from combination therapy ($p<0.05$).

Conclusions The CNVs in plasma cfDNA could predict the clinical outcome of the combination therapy of PD-1 inhibitor with lenvatinib and other ICI-based therapies in hepatobiliary cancers.

INTRODUCTION

Hepatobiliary cancers include a spectrum of lethal carcinomas arising in the liver (hepatocellular carcinoma (HCC)), biliary tract (intrahepatic and extrahepatic cholangiocarcinoma) and gallbladder (gallbladder cancer (GBC)), and many patients are diagnosed with advanced disease.[1 2] Immune checkpoint inhibitor (ICI) therapy or targeted therapy monotherapy has shown considerable efficacy in advanced hepatobiliary cancers.[3–9] Moreover, clinical trials have shown that the combination of ICI therapy with targeted therapy has encouraging efficacy in hepatobiliary cancers.[10–13] The IMbrave150 trial, a phase III randomized study, showed that atezolizumab combined with bevacizumab resulted in better overall survival (OS) and progression-free survival (PFS) than sorafenib in patients with unresectable HCC.[10] Recently, a phase Ib study found that lenvatinib plus a PD-1 inhibitor (pembrolizumab or nivolumab) had a promising objective response rate (ORR) and PFS for unresectable HCC.[11 14] Our previous study indicated that treatment with lenvatinib plus a PD-1 inhibitor is an effective and safe strategy in patients with advanced biliary tract cancer (BTC).[12 13]

However, only a subset of patients benefit from ICI-based therapy. There are no definitive biomarkers for predicting the response to the combination of ICI therapy with targeted therapy in hepatobiliary cancers. Several studies have shown trends toward patients with HCC with positive programmed death-ligand 1 (PD-L1) expression having a higher response to immune checkpoint inhibition monotherapy.[3 15] For BTCs treated with nivolumab, PD-L1 expression was also associated with better PFS and OS.[5] In clinical practice, biomarkers based on tumor tissue have some shortcomings, including the difficulty of obtaining enough tumor tissue as well as spatial heterogeneity. Clinical studies have indicated that cell-free DNA (cfDNA), as a non-invasive tool, provides a promising method for the screening and diagnosis of cancer, the prediction of the response to

therapy, the early diagnosis of relapse and the detection of secondary resistance.[16–18] Moreover, real-time liquid biopsy biomarkers are also expected to assist in clinical decision making, including patient selection and the prediction of immunotherapy efficacy.[19–22]

This study was designed to screen potential biomarkers in plasma cfDNA for predicting the efficacy of the combination therapy of PD-1 inhibitor with lenvatinib and ICI-based therapy in hepatobiliary cancers.

METHODS

Patients

A total of 471 patients with hepatobiliary cancers were screened from two clinical trials (NCT03895970, NCT03892577) at the Peking Union Medical College Hospital. Eligible patients with hepatobiliary cancers who met the inclusion and criteria were recruited to the present study. The main inclusion criteria for patients with hepatobiliary cancer were as follows: (1) pathologically confirmed as hepatobiliary cancer or confirmed by imaging as HCC (by the American Association for the Study of Liver Diseases or standard for the diagnosis and treatment of primary liver cancer 2017 in China)[23 24]; (2) Eastern Cooperative Oncology Group performance status (ECOG PS) score 0–2 and (3) life expectancy of at least 3 months. Two hundred eighty-four patients were excluded based on the following criteria: did not collect blood sample (n=116), blood unmet cfDNA quality (n=41), inadequate organ function (n=34), lacked follow-up data (n=33), organ transplantation status (n=11), active autoimmune disease (n=8), no measurable disease (n=7), died (n=6), withdrew consent (n=13) and excluded for other reasons (n=15). A total of 187 patients with hepatobiliary cancers were divided into three cohorts according to therapy. ICI cohort 1 consisted of 43 patients with hepatobiliary cancers who received combination therapy of PD-1 inhibitor with lenvatinib. ICI cohort 2 included 108 patients with hepatobiliary cancers who received ICI-based therapy. The non-ICI cohort included 36 patients with hepatobiliary cancers who received non-ICI therapy (figure 1).

Assessment of clinical outcomes

The objective response was measured according to the Response Evaluation Criteria in Solid Tumors V.1.1 guidelines,[25] and durable clinical benefit (DCB) was defined as complete response (CR), partial response (PR) or stable disease (SD) for ≥24 weeks,[26] which were evaluated by professional radiologists at our center who were blinded to the therapeutic outcomes and clinicopathological features. For cohort 1 and cohort 2, PFS was defined as the time from the start of anti-PD-1/PD-L1 treatment to the first documented disease progression or death from any cause. OS was defined as the time between the start of anti-PD-1/PD-L1 treatment and death due to any cause. For non-ICI cohort 3, PFS and OS were evaluated as the time from the start of the systematic therapy.

DNA extraction, next-generation sequencing and genomic feature analysis of cfDNA

The plasma cfDNA and blood cell DNA mutation profiles were assessed by a cancer gene-targeted next-generation sequencing (NGS) panel. Methods of DNA extraction, target capture and NGS are provided in the online supplemental material. Algorithm of genomic feature including tumor mutation burden (TMB), copy number instability (CNI) and molecular mutation burden (MMB) are provided in the online supplemental material.

Tumor burden score

The tumor burden score (TBS) was calculated by the maximum tumor size and number of tumors[27 28] using the following formula:

$$TBS^2 = \text{Maximun tumor diameter}^2 + \text{Number of tumors}^2$$

Construction of a prognostic model

A total of 43 patients were randomly allocated to the discovery set (n=30) and validation set (n=13). Univariate Cox regression analysis was performed to analyze the gene copy number value significantly associated with OS. Least absolute shrinkage and selection operator (LASSO) Cox regression analysis was used to determine the coefficient for each feature and estimate the likelihood deviance. The coefficients and partial likelihood deviance were calculated by the 'glmnet' package in R. The copy number variation (CNV) risk score was calculated by the following formula:

$$\text{CNV risk score} = \sum_{i=1}^{n} Coef_i * x_i$$

where $Coef_i$ is the risk coefficient of each factor calculated by the LASSO Cox model, and x_i is the copy number value of each factor.

The time-dependent receiver operating characteristic (tROC) curve to detect the predictive power of the risk score was constructed by the 'survival ROC' package, and Kaplan-Meier analysis with the log-rank test was carried out by the 'survival' package in R. The optimal cut-off value of the CNV risk score was determined by the Youden Index.

Statistical analysis

The clinicopathological features of the discovery and validation cohorts were compared using the χ^2 test (two-tailed). OS and PFS were analyzed by multivariate Cox regression and the Kaplan-Meier method, and the log-rank test was used to detect the significant differences between different groups via the 'survival' and 'survminer' packages in R. The data are expressed as the median and IQR. The Wilcoxon rank-sum test was applied to assess the differences between two groups. Fisher's exact test was used to analyze the correction between CNV risk score with clinicopathological characteristics. P<0.05 was considered significant for two-sided tests. Statistical analyses were performed using R V.3.6.2.

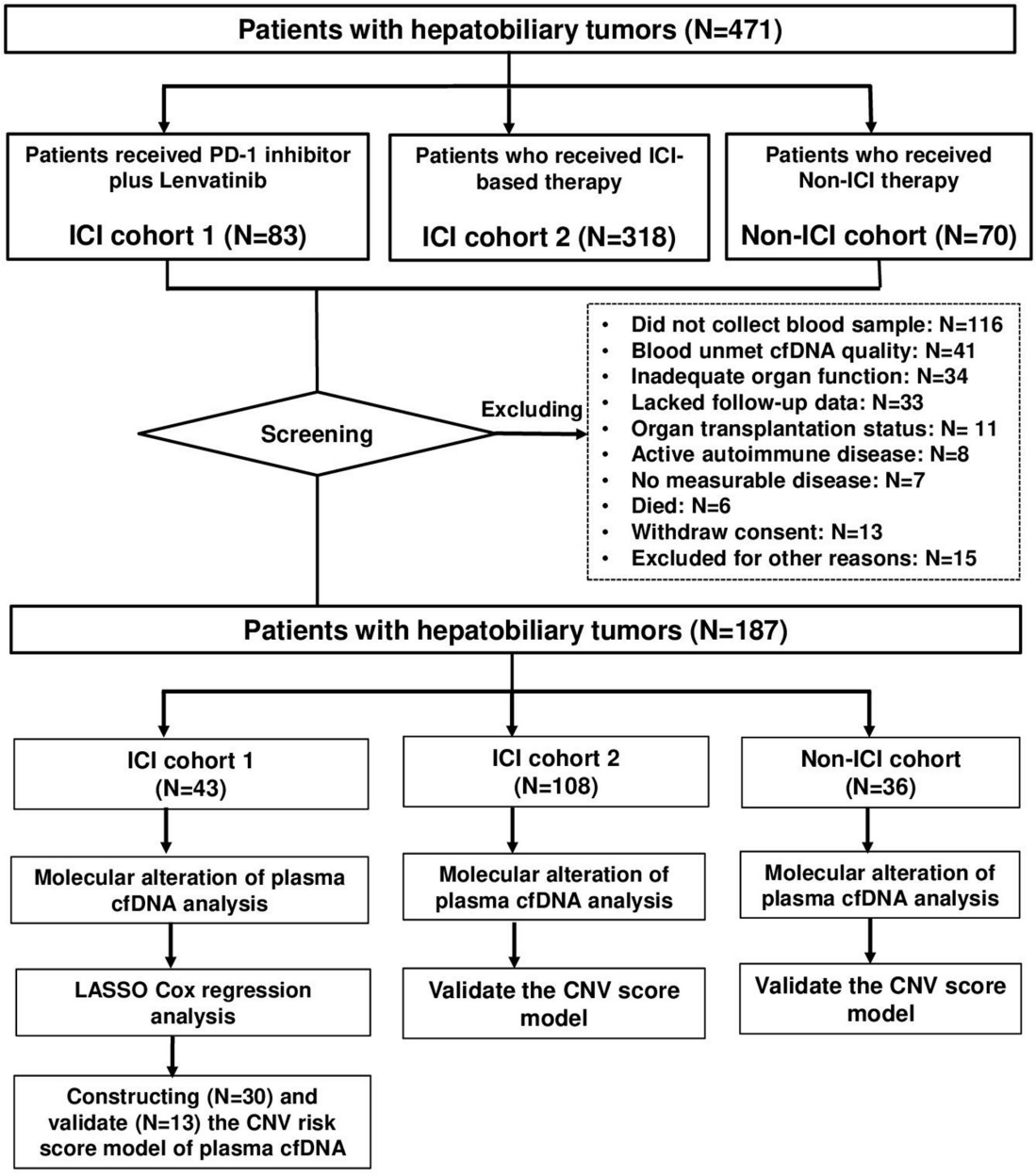

Figure 1 Flow chart of the study design and the data selection process. A total of 471 patients with hepatobiliary cancers were screened. After excluding 284 patients with reasons, three cohorts including 187 patients with hepatobiliary cancers were recruited from clinical trials at the Peking Union Medical College Hospital. Forty-three patients received combination therapy of PD-1 inhibitor with lenvatinib (ICI cohort 1), 108 patients received ICI therapy (ICI cohort 2) and 36 patients received non-ICI therapy (non-ICI cohort). cfDNA, cell-free DNA; CNV, copy number variation; ICI, immune checkpoint inhibitor; LASSO, least absolute shrinkage and selection operator; PD-1, programmed cell death protein 1.

RESULTS

Clinical characteristics of the study cohorts

The detailed clinical characteristics are shown in table 1 and online supplemental table S1. Four hundred seventy-one patients with hepatobiliary cancers were screened, and 284 patients were excluded. Then, a total of 187 patients with hepatobiliary cancers were divided into three cohorts according to therapy. ICI cohort 1 consisted of 43 patients with hepatobiliary cancers who received combination therapy of PD-1 inhibitor with lenvatinib. ICI cohort 1 included 12 patients with HCC, 19 patients with intrahepatic cholangiocarcinoma (ICC), 4 patients with extrahepatic cholangiocarcinoma (ECC), 5 patients with GBC and 3 patients with combined hepatocellular-cholangiocarcinoma (CHCC). The median follow-up was 7.87 months, and 30.2% of 43 patients reached DCB from PD-1 inhibitor plus lenvatinib therapy during the follow-up period. ICI cohort 2 included 108 patients with hepatobiliary cancers who received ICI therapy. ICI cohort 2 included 44 patients with HCC, 39 patients with ICC, 16 patients with ECC, 8 patients with GBC and 1 patient with CHCC. The median follow-up was 11.05 months, and 50% of 108 patients reached DCB from ICI therapy. In the non-ICI cohort, the median follow-up was

Table 1 Key clinical characteristics of patients with hepatobiliary cancer (n=187)

Variable	ICI cohort 1 (n=43)	ICI cohort 2 (n=108)	Non-ICI cohort (n=36)
Median age (range)	61(27–82)	59.5 (18–80)	61.5 (34–84)
Sex—no. (%)			
Male	30 (69.8)	68 (63.0)	26 (72.2)
Female	13 (30.2)	40 (37.0)	10 (27.8)
Histological type—no. (%)			
HCC	12 (27.9)	44 (40.7)	11 (30.6)
ICC	19 (44.2)	39 (36.1)	11 (30.6)
ECC	4 (9.3)	16 (14.8)	7 (19.4)
GBC	5 (11.6)	8 (7.4)	6 (16.7)
CHCC	3 (7.0)	1 (0.9)	1 (2.8)
ECOG PS—no. (%)			
0	25 (58.1)	40 (37.0)	12 (33.3)
1	12 (27.9)	60 (55.6)	18 (50)
2	6 (14.1)	8 (7.4)	6 (16.7)
Child-Pugh grade—no. (%)			
A	38 (88.4)	95 (88.0)	29 (80.6)
B	5 (11.6)	11 (10.2)	5 (13.9)
C	0 (0.0)	2 (1.9)	2 (5.6)
Tumor burden score—no. (%)			
≥8	15 (34.9)	42 (38.9)	10 (27.8)
<8	28 (65.1)	66 (61.1)	26 (72.2)
Number of prior systemic therapies for advanced metastatic disease—no. (%)			
0	28 (65.1)	44 (40.7)	24 (66.7)
1	12 (27.9)	39 (36.1)	4 (11.1)
2 and more	3 (7.0)	25 (23.1)	8 (22.2)
Current therapy—no. (%)			
De novo combination PD-1 inhibitor with lenvatinib	43 (100)	32 (29.6)	0 (0.0)
Lenvatinib sequential PD-1 combination therapy	0 (0.0)	27 (25.0)	0 (0.0)
PD-1 inhibitor+other target therapy	0 (0.0)	49 (45.4)*	0 (0.0)
Target therapy monotherapy	0 (0.0)	0 (0.0)	26 (72.2)†
Others	0 (0.0)	0 (0.0)	10 (27.8)
Follow-up—(IQR) month	7.87 (5.8–11.3)	11.05 (6.68–14.83)	5.83 (3.44–8.26)

*Consists of apatinib (n=23), bevacizumab (n=5) and anlotinib (n=2), regorafenib (n=2), cabozantinib (n=2) and others.
†Lenvatinib (n=16), afatinib (n=2), olaparib (n=2) and others.
CHCC, combined hepatocellular-cholangiocarcinoma; ECC, extrahepatic cholangiocarcinoma; GBC, gallbladder cancer; HCC, hepatocellular carcinoma; ICC, intrahepatic cholangiocarcinoma; ICI, immune checkpoint inhibitor; PD-1, programmed cell death protein 1; PS, performance status.

5.83 months, and 30.6% of 36 patients reached DCB. Sex, histological type and histological grade were comparable among the three cohorts (p>0.05).

Construction and validation of the plasma cfDNA CNV risk score to predict survival after combination therapy

Samples from 187 patients with hepatobiliary cancers were collected. Plasma cfDNA and white blood cell DNA were sequenced by a cancer gene-targeted NGS panel. The mutation profiles of 10 canonical pathways, including the cell cycle, Hippo, Myc, Notch, Nrf2, PI3 kinase/Akt, RTK-RAS, TGFβ signaling, p53 and β-catenin/WNT pathways, were assessed.[29] The *TP53, RICTOR, NF1, CDKN2A, RB1, FBXW7, NFE2L2, PIK3CA, STK11, ERBB4, KRAS* and *NRAS* genes were frequently mutated in hepatobiliary cancers pretreatment (online supplemental figure S1). The landscape of the CNVs in plasma cfDNA is shown in online supplemental figure S2.

Next, we assessed whether the CNVs in plasma cfDNA were predictive of the response to combination therapy of PD-1 inhibitor with lenvatinib. Forty-three patients

were randomly divided into two groups: the discovery cohort (HCC=7, ICC=13, ECC=3 and others=7) and the validation cohort (HCC=5, ICC=6, ECC=1 and GBC=1). Using LASSO Cox regression methods, the genes with CNVs in plasma cfDNA were selected to build the CNV score model to predict survival after combination therapy in the discovery cohort. The formula for the CNV score was based on the copy number of eight genes, including *CALR*, *NR4A3*, *IDH2*, *IGF1R*, *ETV6*, *STAT3*, *NF2* and *CTCF*. The formula for the CNV score was as follows: CNV risk score=(−1.4267831)×*CALR* +0.5515164×*STAT3*+1.5124620×*IDH2*+1.5372432×*ETV6*+4.1835445×*IGF1R*+(−1.3164812)×*NR4A3*+1.1780366×*NF2*+1.5359307×*CTCF* (online supplemental figure S3).

To validate the CNV risk score of plasma cfDNA to predict survival after combination therapy, R packages 'survminer' were used to generate the optimum cut-off value of the CNV score. In the training cohort, we included 30 patients with a CNV risk score of baseline plasma cfDNA higher than 15.68 (high-risk group) with shorter survival times after combination therapy of PD-1 inhibitor with lenvatinib and those with a CNV risk score of baseline plasma cfDNA lower than 15.68 (low-risk group) with longer survival times after combination therapy (figures 2A,C and 3B). We analyzed the CNV risk score and OS of 13 patients from cohort 1 that were not used as part of the training set. The result showed that the patients with high CNV risk score had median OS of 10.37 months and patients with low CNV risk score did not reach (p=0.11) (online supplemental figure 5A). In addition, we compared the CNV risk score between the DCB and no durable benefit (NDB) groups and the CNV risk score among the PR, PD and SD groups, and the results showed the CNV risk score did not significantly change among those groups of 13 patients (online supplemental figure 5B,C). In the validation cohort, the optimum cut-off of the CNV score was the same as that in the discovery cohort, and the results were similar to those in the discovery cohort (figure 2E,F,G). When the distribution of the CNV risk score and survival status were assessed in the training and validation cohorts, the results showed that patients with lower CNV risk scores had better survival than those with higher CNV risk scores (figure 2B,F). The tROC curves of the CNV risk score in the discovery and validation cohorts are shown in figure 4. In the discovery cohort, the CNV risk score had an area under the curve (AUC) of 0.908 at 3 months, 0.847 at 5 months, 0.850 at 10 months and 0.881 at 15 months (figure 2D). In the validation cohort, the CNV risk score had an AUC of 0.867 at 5 months, 0.851 at 10 months and 0.907 at 15 months (figure 2H).

In ICI cohort 1, Kaplan-Meier curves showed that all patients with hepatobiliary cancer with low CNV risk scores (n=20) had longer OS and PFS than patients with hepatobiliary cancer with high CNV risk scores (n=23) (figure 3A, low vs high CNV risk score, PFS: HR=0.39, log-rank p=0.0095; figure 3B, OS: HR=0.045, log-rank p<0.0001). During the follow-up period, the median OS of patients with hepatobiliary cancer with low CNV risk scores was not reached, and the median OS of patients with hepatobiliary cancer with high CNV risk scores was 6.5 months. The median PFS of patients with hepatobiliary cancer with low and high CNV risk scores was 6.17 months and 2.60 months, respectively.

To validate this finding, we further analyzed the 108 patients with hepatobiliary cancer from independent ICI cohort 2 from our clinical trials. The results were similar to those of ICI cohort 1. Favorable OS and PFS were observed in patients with hepatobiliary cancer with low CNV risk scores (figure 3C, low vs high CNV risk score: median PFS, 6.2 months vs 3.03 months, HR=0.61, PFS log-rank p=0.021; figure 3D, median OS, 20.90 months vs 9.80 months, HR=0.50, OS log-rank p=0.015). In the non-ICI cohort, OS and PFS were not significantly different between patients with low and high CNV risk scores (figure 3E,F, PFS log-rank p=0.32, OS log-rank p=0.62).

To further confirm the effect of the CNV risk score of plasma cfDNA at baseline on the OS of patients with hepatobiliary cancer who received combination therapy, multiple Cox regression was used to assess the effect of multiple factors, including cancer type, PD-L1 expression, ECOG score, Child-Pugh score, alpha-fetoprotein (AFP), TBS, macrovascular invasion, etiology, TNM stage and CNV risk score, on OS. The results showed that the CNV risk score of plasma cfDNA was an independent factor for predicting the OS of patients with hepatobiliary cancer who received combination therapy of PD-1 inhibitor with lenvatinib (figure 4, global log-rank p=0.0068; C-index=0.85; CNV risk score: HR=0.021, p=0.009). Using Fisher's exact test in ICI cohorts 1 and 2, we found that the CNV risk score (high/low) was associated with histological type (online supplemental table S2, p<0.05), TBS (online supplemental table S2, p<0.05) and maximum tumor diameter (online supplemental table S2, p<0.05), but not with sex, histological grade or macrovascular invasion (online supplemental table S2, p>0.05).

Association between the plasma cfDNA CNV risk score and the response to ICI therapy

In ICI cohort 1, the CNV risk score of plasma cfDNA was lower in patients showing DCB than in those showing NDB (figure 5A, p=0.042). When the optimum cut-off of the CNV score was used, the result from ICI cohort 1 showed that 53% of patients in the low CNV risk group achieved DCB after combination therapy of PD-1 inhibitor with lenvatinib. In contrast, 12% of patients in the high CNV risk group achieved DCB, and 88% of patients could not benefit from combination therapy of PD-1 inhibitor with lenvatinib (figure 5B, DCB: 53% vs 12%, NDB: 47% vs 88%, p=0.004). In ICI cohort 1, there was a lower tendency of PD and a higher tendency of SD and PR in the low CNV risk group than in the high CNV risk group (figure 5D, PD: 26% vs 52%, SD: 53% vs 38%, PR: 21% vs 10%, p=0.218; disease control rate (DCR), 74% vs 48%, p=0.093). Similar results were

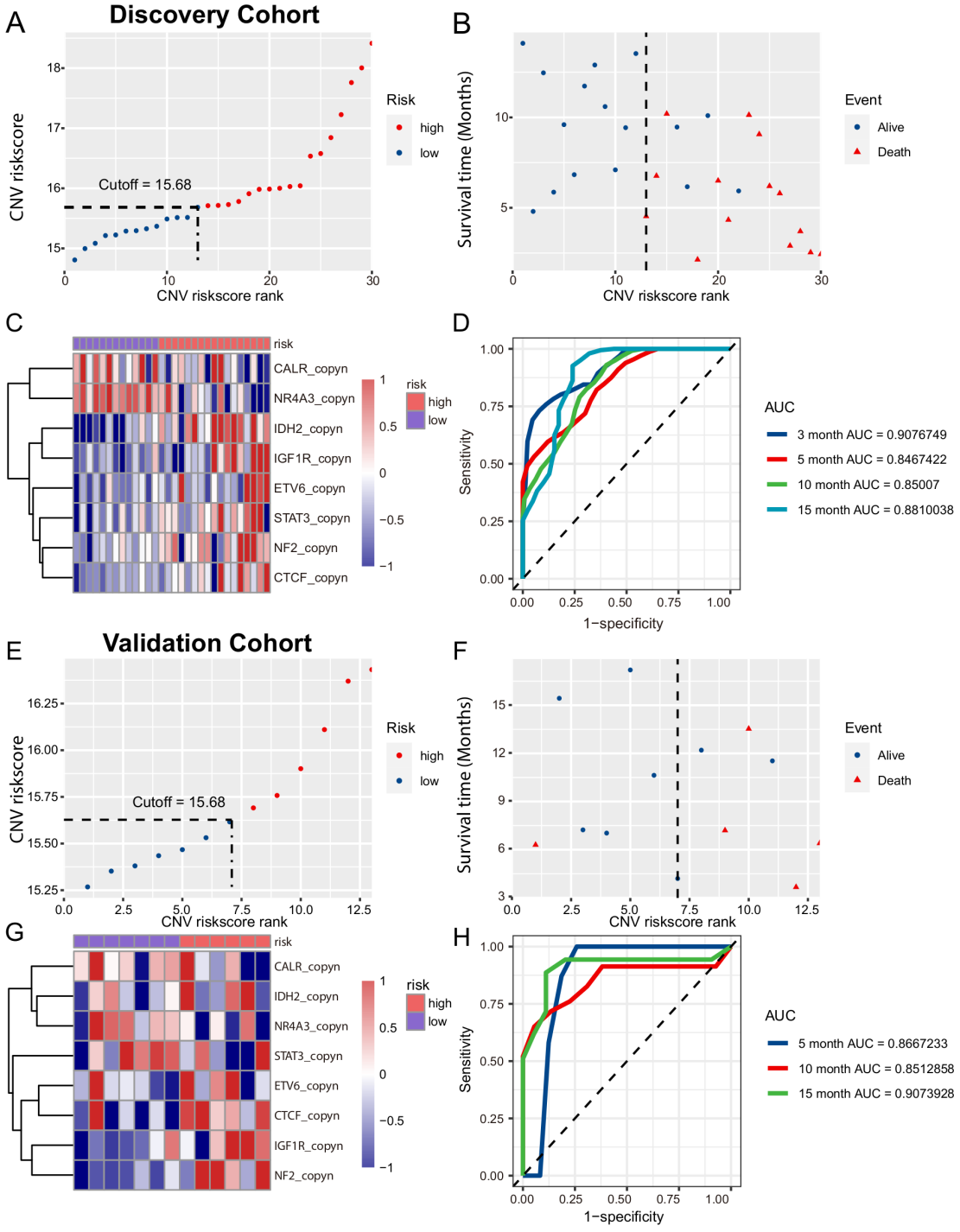

Figure 2 Construction and assessment of the copy number variation (CNV) risk score for hepatobiliary cancers. (A, E) The CNV risk scores of the patients in the discovery and validation cohorts sorted in ascending order. (B, F) Distributions of vital status for each patient according to the CNV risk score levels. (C, G) The copy number Z-scores and level of CNV risk scores of *CALR*, *NR4A3*, *IDH2*, *IGF1R*, *ETV6*, *STAT3*, *NF2* and *CTCF* are shown in the heatmap. (D, H) The area under the curve (AUC) of the time-dependent receiver operating characteristic (ROC) curve was 0.881 in the discovery cohort and 0.907 in the validation cohort for the CNV risk score.

observed in ICI cohort 2. The CNV risk score of plasma cfDNA was lower in patients showing DCB than in those showing NDB (figure 5E, p=0.0023). Compared with that in the high CNV risk group, a higher percentage of patients in the low CNV risk group achieved DCB after ICI therapy (figure 5F; DCB: 64% vs 37%, NDB: 36% vs 63%, p=0.005). The CNV risk score was higher in the PD group than in the SD and PR groups in both ICI cohort 1 and ICI cohort 2 (figure 5C,G; ICI cohort 1: PD vs SD, p=0.039, PD vs PR, not significant; ICI cohort 2: PD vs SD, p=0.0067, PD vs PR, p=0.027). In ICI cohort 2, the percentage of PD was significantly lower and the

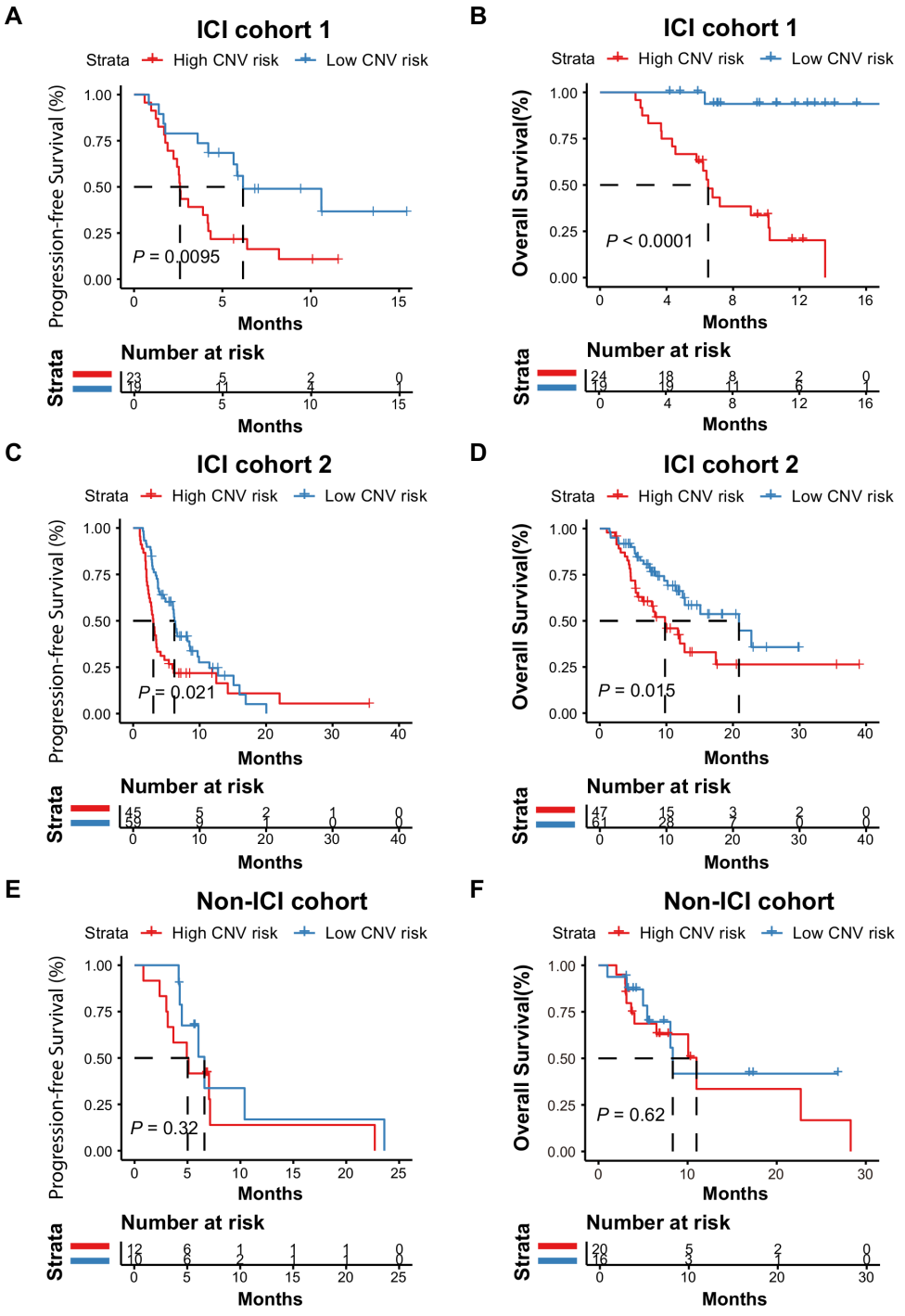

Figure 3 Association between the plasma cell-free DNA (cfDNA) copy number variation (CNV) risk score and the response to immune checkpoint inhibitor (ICI) therapy. (A and B) Kaplan-Meier curves for the overall survival (OS) and progression-free survival (PFS) of patients with hepatobiliary cancer in ICI cohort 1 stratified into high CNV risk and low CNV risk score groups. The PFS log-rank test showed p=0.0095; low versus high CNV risk, median PFS: 6.17 months vs 2.60 months, HR=0.045. The OS log-rank test showed p<0.0001; low vs high CNV risk, median OS: not reached vs 6.5 months, HR=0.39. (C and D) Kaplan-Meier curves for the PFS and OS of patients with hepatobiliary cancer in ICI cohort 2 stratified into high CNV risk and low CNV risk score groups. The log-rank test of PFS in different CNV risk score groups showed p=0.021; low versus high CNV risk score: median PFS, 6.2 months vs 3.033 months, HR=0.61. The OS log-rank test showed p=0.015; low vs high CNV risk score: median OS, 20.9 months vs 9.8 months, HR=0.50. (E and F) Kaplan-Meier curves for the PFS and OS of patients with hepatobiliary cancer in the non-ICI cohort stratified into high CNV risk and low CNV risk score groups. The PFS log-rank test showed p=0.32; low versus high CNV risk, median PFS: 6.60 months vs 5.02 months. The OS log-rank test showed p=0.62, low versus high CNV risk, median OS: 8.33 months vs 1.00 months.

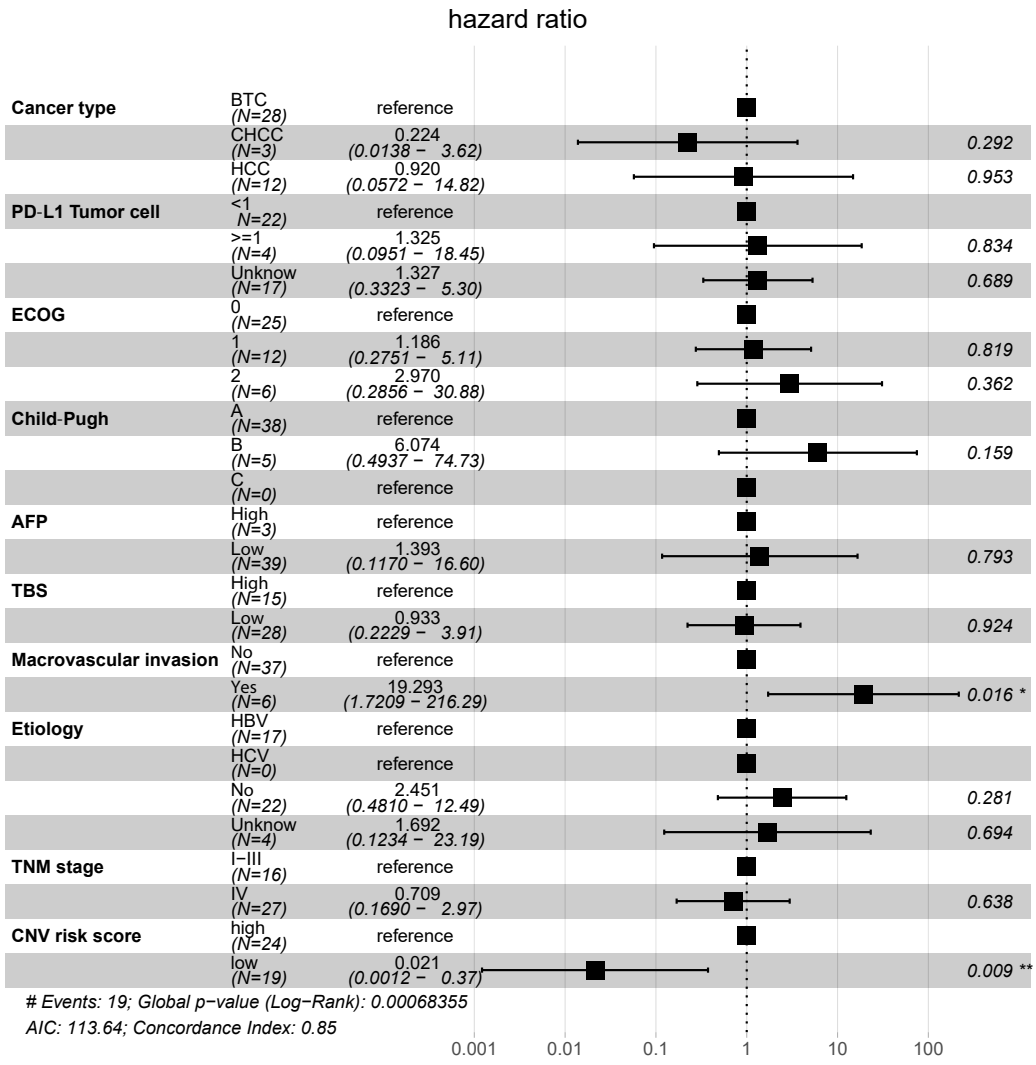

Figure 4 Effect of the copy number variation (CNV) risk score on overall survival after combination therapy of programmed cell death protein 1 (PD-1) inhibitor with lenvatinib, by clinical characteristics. Forest plot for overall survival in subgroups. Estimates are based on a Cox proportional hazards model. AFP, alpha-fetoprotein; ECOG, Eastern Cooperative Oncology Group; PD-L1, programmed death-ligand 1; TBS, tumor burden score; TNM, tumor, node, metastases.

percentages of SD and PR were significantly higher in the low CNV risk group than in the high CNV risk group (figure 5H, PR: 15% vs 20%, SD: 69% vs 47%, PD: 15% vs 33%, p=0.046; DCR: 85% vs 63%, p=0.011).

The molecular features of hepatobiliary cancers with high and low CNV risk scores were investigated. Hepatobiliary cancers with high CNV risk scores were characterized by high TMB and MMB. Moreover, higher CNI scores were observed in hepatobiliary cancers with high CNV risk scores than in hepatobiliary cancers with low CNV risk scores (online supplemental figure S4, p<0.05).

DISCUSSION

ICI-based therapy may provide new clinical strategies for patients with hepatobiliary cancers. This study constructed a CNV risk score model of plasma cfDNA to predict the clinical outcome of the combination therapy of PD-1 inhibitor with lenvatinib and other ICI-based therapies in hepatobiliary cancers.

Chromosomal instability is a hallmark of cancer biology.[30] Several studies have indicated that CNVs identified in tumor tissue is related to the response to immunotherapy in patients with cancer.[31–34] A recent study found that HCC tumors with a low burden of broad copy number chromosomal alterations display higher immune infiltration and have a better response rate to anti-PD-1 inhibitors than those with a median/high broad copy number.[35] Moreover, Davoli *et al*[31] found that a higher CNV burden in tumor tissue correlated with immune escape and poorer survival in patients with metastatic melanoma treated with immunotherapy. Regarding liquid biopsy, Weiss *et al*[36] constructed a CNI scoring system based on plasma cfDNA and found that the CNI score could be used as an early indicator of the response

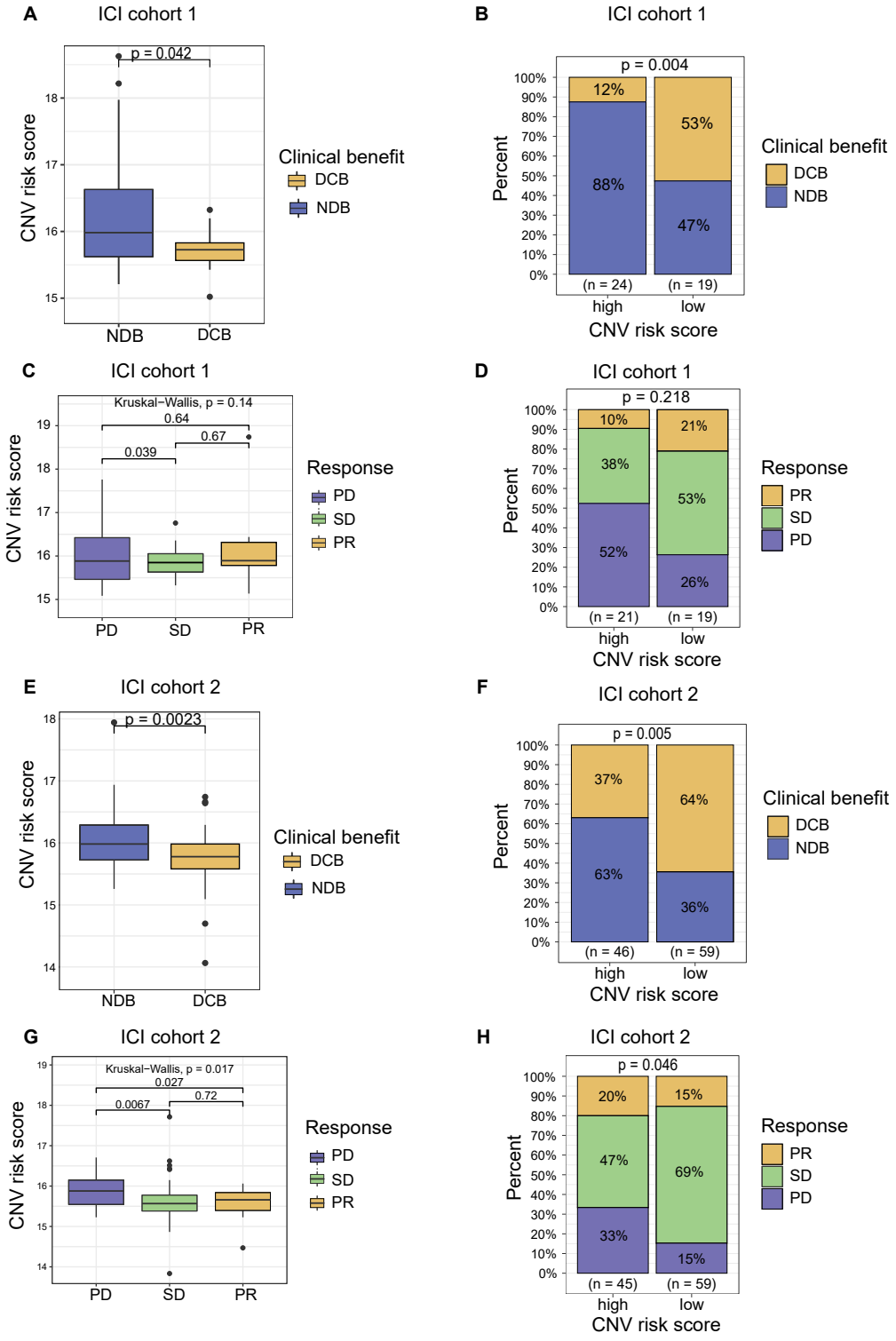

Figure 5 Association between the copy number variation (CNV) risk score of plasma cell-free DNA (cfDNA) and the response to immune checkpoint inhibitor (ICI)-based therapy. (A) CNV risk score levels of patients in the durable clinical benefit (DCB) and no durable benefit (NDB) groups from ICI cohort 1. (B) Proportional representation of DCB and NDB in ICI cohort 1 based on the level of the CNV risk score. (C) The CNV risk score levels of patients in the partial response (PR), stable disease (SD) and progressive disease (PD) groups from ICI cohort 1. (D) Proportional representation of the objective response rate (ORR) in ICI cohort 1 based on level of the CNV risk score. (E) CNV risk score levels of patients in the DCB and NDB groups from ICI cohort 2. (F) Proportional representation of DCB and NDB in ICI cohort 2 based on the level of the CNV risk score. (G) CNV risk score levels of patients in the PR, SD and PD groups from ICI cohort 2. (H) Proportional representation of the ORR in ICI cohort 2 based on the level of the CNV risk score.

to immunotherapy for diverse advanced cancers. Another study also found that the cfDNA genome instability number (GIN) could discriminate atypical responses (such as pseudoprogression or hyperprogressive disease) and could monitor the response to ICI therapy.[37] However, the association between CNV and immunotherapy in hepatobiliary cancer is still unclear. In this study, by using LASSO Cox regression, we constructed a CNV risk score model to predict the response to combination therapy. The results of the tROC analysis were encouraging, and the CNV risk score had an AUC >0.8. In the PD-1 inhibitor and lenvatinib combination therapy cohort, favorable OS and PFS were observed in patients with hepatobiliary cancer with low CNV risk scores. These results were confirmed in another independent ICI-based cohort of patients with hepatobiliary cancer. These findings are based on pretreatment plasma cfDNA alterations, which could provide new biomarkers and information for clinicians to make appropriate clinical decisions for each patient. In the non-ICI cohort, the CNV risk score was not associated with the clinical outcome of patients. Our findings indicated that the patients with hepatobiliary cancers with low cfDNA CNV risk score benefit from the PD-1 inhibitor with lenvatinib and other ICI-based therapies. In addition, we further investigated the molecular features of tumors with low and high CNV risk scores, and the results showed that tumors with high CNV risk scores were characterized as highly malignant, as reflected by the TMB, MMB and CNI score. A recent study reported that HCC with high broad CNV score showed high mutational burdens,[35] which was similar to our study. In addition, this study indicated that patients with HCC with high broad CNV scores had lower ratio of observed/expected neoantigens. It suggested that the accumulation of CNV may be associated with an enhanced editing of non-antigenic mutations, regardless of overall mutation burdens.[35] These findings may explain the poor clinical outcome of patients with tumors with high CNV risk scores treated with ICI-based therapy.

Although ICI-based therapy has led to evolutionary developments in cancer management, some patients still do not respond to therapy. In our PD-1 inhibitor and lenvatinib combination therapy cohort, 30.2% of patients achieved DCB from combination therapy, and 69.8% of patients could not benefit from the combination therapy. In clinical practice, the main concern is selecting patients who would benefit from the therapy. Meanwhile, excluding patients who would not benefit from therapy is also equally important. In our study, we found that >50% of patients with low CNV risk scores achieved DCB from combination therapy. In contrast, only 12% of patients with high CNV risk scores achieved DCB from combination therapy, and 88% of patients with high CNV risk scores could not benefit from combination therapy. Our findings suggested that patients with low CNV risk scores were more likely to benefit from combination therapy; in contrast, patients with high CNV risk scores were less likely to benefit from combination therapy.

There were several limitations in the present study. This is a single-center retrospective study and the cohorts were relatively heterogeneous among cancer types or ICI-based regimens. Moreover, this CNV risk score model was constructed based on a small number of patients, therefore, further larger independent studies and multicenter should be designed to validate the clinical value of plasma cfDNA CNVs in predicting immunotherapy efficacy in hepatobiliary cancers.

CONCLUSIONS

In summary, the present study constructed a CNV risk score model based on plasma cfDNA to predict survival after combination therapy of PD-1 inhibitor with lenvatinib and other ICI-based therapies in hepatobiliary cancers. In clinical practice, the cfDNA CNV risk score may provide valuable resources for personalized hepatobiliary cancer combination immunotherapy regimens.

Author affiliations
[1]Department of Liver Surgery, State Key Laboratory of Complex Severe and Rare Diseases, Peking Union Medical College Hospital, Chinese Academy of Medical Sciences and Peking Union Medical College, Beijing, China
[2]Center of Integrative Medicine, Beijing Ditan Hospital, Capital Medical University, Beijing, China
[3]Genecast Biotechnology Co., Ltd, Wuxi, China
[4]Department of Medical Oncology, Peking Union Medical College Hospital, Chinese Academy of Medical Sciences and Peking Union Medical College, Beijing, China
[5]Department of Radiology, Peking Union Medical College Hospital, Chinese Academy of Medical Sciences and Peking Union Medical College, Beijing, China
[6]Department of Nuclear Medicine, Peking Union Medical College Hospital, Chinese Academy of Medical Sciences and Peking Union Medical College, Beijing, China
[7]Center of Radiotherapy, Peking Union Medical College Hospital, Chinese Academy of Medical Sciences and Peking Union Medical College, Beijing, China
[8]Department of Immunology, School of Basic Medical Sciences, Capital Medical University, Beijing, China
[9]Beijing Shijitan Hospital, Capital Medical University, Beijing, China; Ninth School of Clinical Medicine, Peking University, Beijing, China; School of Oncology, Capital Medical University, Beijing, China
[10]Institute of Infectious Diseases, Beijing Ditan Hospital, Capital Medical University, Beijing, China

Acknowledgements The authors would like to thank all the participating patients and their families.

Contributors HZhao, HZhang, XuY and YH designed the study. XuY, YH, KY, DW, JLin, JLong, FX, JM, JB, MG, JP, LH, KH, XiaoboY, and JZ were involved in acquisition, analysis, and interpretation of data. HZhao, HZhang, XW, XuY, DW, YH and KY explained the results and wrote the manuscript. HZhao, HZhang, XW, YM, XS, and XiaoboY provided critical revision of the manuscript. All authors read and approved the final manuscript.

Funding This work was supported by the International Science and Technology Cooperation Projects (2016YFE0107100), CAMS Clinical and Translational Medicine Research Funds (2019XK320006), National Ten-thousand Talent Program and National Key Sci-Tech Special Project of China (2018ZX10302207).

Competing interests None declared.

Patient consent for publication Not required.

Ethics approval The study protocol was approved by the institutional review board and ethics committee of the Peking Union Medical College Hospital (JS-1391 and JS-1864), and all patients provided written informed consent.

Provenance and peer review Not commissioned; externally peer reviewed.

Data availability statement Data are available on reasonable request.

ORCID iD

Haitao Zhao http://orcid.org/0000-0002-3444-8044

REFERENCES

1 Benson AB, D'Angelica MI, Abbott DE, *et al*. Guidelines insights: hepatobiliary cancers, version 2.2019. *J Natl Compr Canc Netw* 2019;17:302–10.
2 Lin J, Shi J, Guo H, *et al*. Alterations in DNA damage repair genes in primary liver cancer. *Clin Cancer Res* 2019;25:4701–11.
3 Sangro B, Park J, Finn R, *et al*. LBA-3 CheckMate 459: long-term (minimum follow-up 33.6 months) survival outcomes with nivolumab versus sorafenib as first-line treatment in patients with advanced hepatocellular carcinoma. *Ann Oncol* 2020;31:S241–2.
4 Finn RS, Ryoo B-Y, Merle P, *et al*. Pembrolizumab as second-line therapy in patients with advanced hepatocellular carcinoma in KEYNOTE-240: a randomized, double-blind, phase III trial. *J Clin Oncol* 2020;38:Jco1901307.
5 Kim RD, Chung V, Alese OB, *et al*. A phase 2 multi-institutional study of nivolumab for patients with advanced refractory biliary tract cancer. *JAMA Oncol* 2020;6:888–8.
6 Kudo M, Finn RS, Qin S, *et al*. Lenvatinib versus sorafenib in first-line treatment of patients with unresectable hepatocellular carcinoma: a randomised phase 3 non-inferiority trial. *Lancet* 2018;391:1163–73.
7 Ikeda M, Sasaki T, Morizane C, *et al*. A phase 2 study of lenvatinib monotherapy as second-line treatment in unresectable biliary tract cancer: primary analysis results. *Ann Oncol* 2017;28:v246.
8 Wang D, Lin J, Yang X, *et al*. Combination regimens with PD-1/PD-L1 immune checkpoint inhibitors for gastrointestinal malignancies. *J Hematol Oncol* 2019;12:42.
9 Yoo C, Oh D-Y, Choi HJ, *et al*. Phase I study of bintrafusp alfa, a bifunctional fusion protein targeting TGF-β and PD-L1, in patients with pretreated biliary tract cancer. *J Immunother Cancer* 2020;8:e000564.
10 Finn RS, Qin S, Ikeda M, *et al*. Atezolizumab plus bevacizumab in unresectable hepatocellular carcinoma. *N Engl J Med* 2020;382:1894–905.
11 Kudo M, Ikeda M, Motomura K, *et al*. A phase Ib study of lenvatinib (LEN) plus nivolumab (NIV) in patients (PTS) with unresectable hepatocellular carcinoma (uHCC): study 117. *JCO* 2020;38:513.
12 Lin J, Yang X, Zhao S, *et al*. Lenvatinib plus PD-1 blockade in advanced bile tract carcinoma. *Ann Oncol* 2019;30:v517.
13 Lin J, Yang X, Long J, *et al*. Pembrolizumab combined with lenvatinib as non-first-line therapy in patients with refractory biliary tract carcinoma. *Hepatobiliary Surg Nutr* 2020;9:414–24.
14 Finn RS, Ikeda M, Zhu AX, *et al*. Phase Ib study of lenvatinib plus pembrolizumab in patients with unresectable hepatocellular carcinoma. *J Clin Oncol* 2020;38:2960–70.
15 Sangro B, Melero I, Wadhawan S, *et al*. Association of inflammatory biomarkers with clinical outcomes in nivolumab-treated patients with advanced hepatocellular carcinoma. *J Hepatol* 2020;73:1460–9.
16 Christensen E, Birkenkamp-Demtröder K, Sethi H, Shchegrova S, *et al*. Early detection of metastatic relapse and monitoring of therapeutic efficacy by Ultra-Deep sequencing of plasma cell-free DNA in patients with urothelial bladder carcinoma. *J Clin Oncol* 2019;37:1547–57.
17 Cai J, Chen L, Zhang Z, *et al*. Genome-Wide mapping of 5-hydroxymethylcytosines in circulating cell-free DNA as a non-invasive approach for early detection of hepatocellular carcinoma. *Gut* 2019;68:2195–205.
18 Cristiano S, Leal A, Phallen J, *et al*. Genome-Wide cell-free DNA fragmentation in patients with cancer. *Nature* 2019;570:385–9.
19 Cabel L, Proudhon C, Romano E, *et al*. Clinical potential of circulating tumour DNA in patients receiving anticancer immunotherapy. *Nat Rev Clin Oncol* 2018;15:639–50.
20 Lipson EJ, Velculescu VE, Pritchard TS, *et al*. Circulating tumor DNA analysis as a real-time method for monitoring tumor burden in melanoma patients undergoing treatment with immune checkpoint blockade. *J Immunother Cancer* 2014;2:42.
21 Giroux Leprieur E, Hélias-Rodzewicz Z, Takam Kamga P, *et al*. Sequential ctDNA whole-exome sequencing in advanced lung adenocarcinoma with initial durable tumor response on immune checkpoint inhibitor and late progression. *J Immunother Cancer* 2020;8:e000527.
22 Forschner A, Battke F, Hadaschik D, *et al*. Tumor mutation burden and circulating tumor DNA in combined CTLA-4 and PD-1 antibody therapy in metastatic melanoma - results of a prospective biomarker study. *J Immunother Cancer* 2019;7:180.
23 Heimbach JK, Kulik LM, Finn RS, *et al*. AASLD guidelines for the treatment of hepatocellular carcinoma. *Hepatology* 2018;67:358–80.
24 Zhou J, Sun H-C, Wang Z, *et al*. Guidelines for diagnosis and treatment of primary liver cancer in China (2017 edition). *Liver Cancer* 2018;7:235–60.
25 Schwartz LH, Litière S, de Vries E, *et al*. RECIST 1.1-Update and clarification: from the RECIST committee. *Eur J Cancer* 2016;62:132–7.
26 Quispel-Janssen J, van der Noort V, de Vries JF, *et al*. Programmed death 1 blockade with nivolumab in patients with recurrent malignant pleural mesothelioma. *J Thorac Oncol* 2018;13:1569–76.
27 Sasaki K, Morioka D, Conci S, *et al*. The Tumor Burden Score: A New "Metro-ticket" Prognostic Tool For Colorectal Liver Metastases Based on Tumor Size and Number of Tumors. *Ann Surg* 2018;267:132–41.
28 Vitale A, Lai Q, Farinati F, *et al*. Utility of tumor burden score to stratify prognosis of patients with hepatocellular cancer: results of 4759 cases from ITA.LI.CA Study Group. *J Gastrointest Surg* 2018;22:859–71.
29 Sanchez-Vega F, Mina M, Armenia J, *et al*. Oncogenic signaling pathways in the cancer genome atlas. *Cell* 2018;173:321–37.
30 Hanahan D, Weinberg RA. Hallmarks of cancer: the next generation. *Cell* 2011;144:646–74.
31 Davoli T, Uno H, Wooten EC, *et al*. Tumor aneuploidy correlates with markers of immune evasion and with reduced response to immunotherapy. *Science* 2017;355(6322) (published Online First: 2017/01/21).
32 Roh W, Chen P-L, Reuben A, *et al*. Integrated molecular analysis of tumor biopsies on sequential CTLA-4 and PD-1 blockade reveals markers of response and resistance. *Sci Transl Med* 2017;9:eaah3560.
33 Liu L, Bai X, Wang J, *et al*. Combination of TMB and CNA Stratifies prognostic and predictive responses to immunotherapy across metastatic cancer. *Clin Cancer Res* 2019;25:7413–23.
34 Lu Z, Chen H, Li S, *et al*. Tumor copy-number alterations predict response to immune-checkpoint-blockade in gastrointestinal cancer. *J Immunother Cancer* 2020;8:e000374.
35 Bassaganyas L, Pinyol R, Esteban-Fabró R, *et al*. Copy-Number alteration burden differentially impacts immune profiles and molecular features of hepatocellular carcinoma. *Clin Cancer Res* 2020;26:6350–61.
36 Weiss GJ, Beck J, Braun DP, *et al*. Tumor cell-free DNA copy number instability predicts therapeutic response to immunotherapy. *Clin Cancer Res* 2017;23:5074–81.
37 Jensen TJ, Goodman AM, Kato S, *et al*. Genome-Wide sequencing of cell-free DNA identifies copy-number alterations that can be used for monitoring response to immunotherapy in cancer patients. *Mol Cancer Ther* 2019;18:448–58.

Supplementary Methods

Cell-free DNA copy number variations predict efficacy of immune checkpoint inhibitor-based therapy in hepatobiliary cancers

DNA extraction

Whole blood samples were centrifuged in Streck tubes at 1600 x g for 10 minutes at room temperature to separate plasma. The upper plasma layer was removed and transferred to a new 1.5 mL tube, followed by centrifugation of the plasma at 16000 x g for 10 minutes at room temperature. Plasma cell-free DNA (cfDNA) was isolated using the MagMAX Cell-free DNA Isolation Kit (Life Technologies, California, USA) according to the manufacturer's instructions. To isolate genomic DNA (gDNA), we centrifuged whole blood and collected the buffy coat layer to separate the white blood cell samples, and then we used the TIANamp Genomic DNA Kit (Tiangen, Beijing, China) according to the manufacturer's protocol. The concentrations of purified DNA were determined by the Qubit dsDNA HS Assay Kit with the Qubit 4.0 Fluorometer (Life Technologies, California, USA).

Library construction, target capture and next-generation sequencing

The plasma cfDNA and blood cell DNA mutation profiles were assessed by a cancer gene–targeted NGS panel in Genecast Biotechnology Co Ltd China laboratory. The cancer gene-targeted NGS was designed by Genecast and commercially available(Genecast, Wuxi, China). Genomic DNA was sheared into 150-200 bp fragments with a Covaris M220 Focused-ultrasonicator instrument (Covaris, Massachusetts, USA). Fragmented gDNA and cfDNA libraries were constructed by the KAPA Hyper Prep Kit (Kapa Biosystems, Massachusetts, USA) according to the manufacturer's instructions. The concentrations and size distributions of the libraries were analysed by a Qubit 4.0 Fluorometer (Life Technologies, California, USA) and an Agilent Bioanalyzer 2100 (Agilent Technologies, USA). DNA libraries were captured

following the NimbleGen SeqCap EZ Library SR (Roche, Wisconsin, USA) User's Guide with a designed Genescope panel (Genecast, Wuxi, China) that included major tumour-related genes. The captured libraries were sequenced with the Illumina NovaSeq 6000 platform (Illumina, California, USA) to produce 150 paired-end sequences according to the manufacturer's instructions.

Mapping and single-nucleotide variant (SNV) and copy number variation (CNV) calling

The SNV and CNV calling of cfDNA was according to the standard pipeline in previously published study which also used the Genecast's cancer gene–targeted NGS panel.[1] The paired-end reads generated from the NovaSeq 6000 platform were mapped to the hg19 reference genome (NCBI Build 37.5) with BWA 0.7.17 version (default parameters)[2]. Then, the Picard toolkit (v 2.1.0) and Genome Analysis ToolKit (v 3.7) were used to make duplicates and for realignment.VarDict (v 1.5.1)[3] was used for variant calling to plasma samples and matched white blood cell samples of each patient, while compound heterozygous mutations were merged by FreeBayes (v 1.2.0)[4]. After annotation through ANNOVAR[5], somatic mutations were selected using the following criteria: i) located in intergenic or intronic regions; ii) identified as synonymous SNVs; iii) allele frequency >= 0.002 in the Exome Aggregation Consortium (ExAC)[6] and gnomAD databases; iv) allele frequency <0.01 in plasma samples; v) strand bias mutations in the reads; vi) support reads <5; and vii) depth <30.

For CNV calling, we used 30 health control blood samples to construct copy number baseline as negative control and used software ctCNV to call copy number variation for each case. First, counting the read count for each target region and normalize the read count for all regions of each sample so that the different samples are comparable. Second, applying rolling median to normalize GC-content and length of target regions. After correcting GC content, target region length, and read count, normalized test samples are compared to the baseline, log2ratios are calculated at each region-level first, and then the median of log2ratios of all regions within the same gene range is used to

represent the log2ratio of the gene. To determine the CNV for each gene, in addition to the absolute copy number, we also calculated the gene specificity score (GCS, represents the degree of gene level difference between the test sample and control), with quantitate the instability of copy number compare to the control samples, and added a statistical test filter to determine whether the GCS is significantly different from control samples. Only genes who are statistically significant and absolute copy number exceed a given threshold will be judged to be CNV.

To determine the copy number, we used white blood cell samples as a negative control and used cnvkit (v 0.9.2) software to call the CNVs from the matched plasma samples of patients[7].

Molecular features

The number of somatic nonsynonymous SNVs in all samples were determined to calculate the tumour mutation burden (TMB) with the following rules: i) not splicing or exonic; ii) sequencing depth <100X and allele frequency < 0.05; iii) allele frequency >=0.002 in the ExAC[6] and gnomAD databases; and iv) strand bias mutations in the reads and other rules. The TMB of the samples was calculated by the absolute mutation counts via the following formula:

$$TMB = \frac{Absolute\ mutation\ counts}{Panel\ exonic\ base\ num} \times 1000000$$

TMB was measured in mutations per Mb[8].

The copy number instability (CNI) score was calculated by the sum of the Z-scores computed by the following step. The log2 read counts were converted into Z-scores based on Gaussian transformations versus a normal control group after the correction of GC content and length of target region using proprietary algorithms for each region. If the Z-score was greater than the 95th percentile plus twice the absolute standard deviation of the normal control group, the target regions were retained and summed into the CNI score [9].

Molecular mutation burden (MMB) was calculated by the mean frequency among the obtained mutations for each gene of each patient. Details could be seen in the previous study.[10]

The somatic mutations of ten oncogenic signalling pathways, including the cell cycle, Hippo, Myc, Notch, Nrf2, PI-3-Kinase/Akt, RTK-RAS, TGFβ signalling, p53 and β-catenin/Wnt pathways, were analysed as described in a previous publication.[11]

Supplementary References

1. Jiang T, Jiang L, Dong X, et al. Utilization of circulating cell-free DNA profiling to guide first-line chemotherapy in advanced lung squamous cell carcinoma. *Theranostics* 2021;11(1):257-67. doi: 10.7150/thno.51243 [published Online First: 2021/01/05]
2. Li H, Durbin R. Fast and accurate short read alignment with Burrows-Wheeler transform. *Bioinformatics* 2009;25(14):1754-60. doi: 10.1093/bioinformatics/btp324 [published Online First: 2009/05/20]
3. Lai Z, Markovets A, Ahdesmaki M, et al. VarDict: a novel and versatile variant caller for next-generation sequencing in cancer research. *Nucleic Acids Res* 2016;44(11):e108. doi: 10.1093/nar/gkw227 [published Online First: 2016/04/10]
4. Garrison E, Marth G. Haplotype-based variant detection from short-read sequencing. *arXiv* 2012;preprint arXiv:1207.3907
5. Wang K, Li M, Hakonarson H. ANNOVAR: functional annotation of genetic variants from high-throughput sequencing data. *Nucleic Acids Res* 2010;38(16):e164. doi: 10.1093/nar/gkq603 [published Online First: 2010/07/06]
6. Karczewski KJ, Weisburd B, Thomas B, et al. The ExAC browser: displaying reference data information from over 60 000 exomes. *Nucleic Acids Res* 2017;45(D1):D840-d45. doi: 10.1093/nar/gkw971 [published Online First: 2016/12/03]
7. Talevich E, Shain AH, Botton T, et al. CNVkit: Genome-Wide Copy Number Detection and Visualization from Targeted DNA Sequencing. *PLoS Comp Biol* 2016;12(4):e1004873. doi: 10.1371/journal.pcbi.1004873 [published Online First: 2016/04/23]
8. Chalmers ZR, Connelly CF, Fabrizio D, et al. Analysis of 100,000 human cancer genomes reveals the landscape of tumor mutational burden. *Genome Med* 2017;9(1):34. doi: 10.1186/s13073-017-0424-2 [published Online First: 2017/04/20]
9. Weiss GJ, Beck J, Braun DP, et al. Tumor Cell-Free DNA Copy Number Instability Predicts Therapeutic Response to Immunotherapy. *Clin Cancer Res* 2017;23(17):5074-81. doi: 10.1158/1078-0432.Ccr-17-0231 [published Online First: 2017/03/23]
10. Jiang T, Li X, Wang J, et al. Mutational Landscape of cfDNA Identifies Distinct Molecular Features Associated With Therapeutic Response to First-Line Platinum-Based Doublet Chemotherapy in Patients with Advanced NSCLC. *Theranostics* 2017;7(19):4753-62. doi: 10.7150/thno.21687 [published Online First: 2017/12/01]
11. Sanchez-Vega F, Mina M, Armenia J, et al. Oncogenic Signaling Pathways in The Cancer Genome Atlas. *Cell* 2018;173(2):321-37.e10. doi: 10.1016/j.cell.2018.03.035 [published Online First: 2018/04/07]

Supplementary Table 1. Other clinical characteristics of patients with hepatobiliary cancer (N = 187)

Variable	ICI cohort 1 (N=43)	ICI Cohort2 (N=108)	Non-ICI Cohort (N=36)
Etiology — no. (%)			
Hepatitis B	**17(39.5)**	**46(42.6)**	**10(27.8)**
Hepatitis C	**0(0)**	**3(2.8)**	**2(5.6)**
NAFLD	**2(4.7)**	**6(5.6)**	**1(2.8)**
AFLD	**3(7.0)**	**4(3.7)**	**1(2.8)**
Alcohol use	**3(7.0)**	**8(7.4)**	**1(2.8)**
Others	**24(55.8)**	**53(49.0)**	**23(63.8)**
Biliary stone — no. (%)			
Y	**9(20.9)**	**27(25.0)**	**8(22.2)**
N	**32(74.4)**	**78(72.2)**	**24(66.7)**
NA	**2(4.7)**	**3(2.8)**	**4(11.1)**
Macrovascular Invasion — no. (%)			
Y	**6(14.0)**	**26(24.1)**	**3(8.3)**
N	**37(86.0)**	**82(75.9)**	**33(91.7)**
TNM Stage — no. (%)			
I	**0 (37.2)**	**2 (1.9)**	**4(11.1)**
II	**6(14.0)**	**9(8.3)**	**5(13.9)**
III	**10(23.3)**	**32(29.6)**	**10(27.8)**
IV	**27(62.8)**	**65(60.2)**	**17(47.2)**
Distant metastasis — no. (%)			
Y	**23(53.5)**	**50(46.3)**	**15(41.7)**
N	**20(46.5)**	**58(53.7)**	**21(58.3)**
ALBI score — no. (%)			
1	**30(69.8)**	**72(66.7)**	**21(58.3)**
2	**13(30.2)**	**33(30.6)**	**12(33.3)**
3	**0(0.0)**	**3(2.8)**	**3(8.3)**
AFP>400ng/ml — no. (%)			
Y	**3(7.0)**	**16(14.8)**	**4(11.1)**
N	**39(90.7)**	**88(81.5)**	**32(88.9)**
NA	**1(2.3)**	**4(3.7)**	**0(0.0)**
CA19-9>100U/L — no. (%)			
Y	**18(41.9)**	**42(38.9)**	**11(30.6)**
N	**24(55.8)**	**63(58.3)**	**25(69.4)**
NA	**1(2.3)**	**3(2.8)**	**0(0.0)**
Maximum tumor diameter — no. (%)			
>=5 cm	**25(58.1)**	**54(50.0)**	**11(30.6)**

Variable	ICI cohort 1 (N=43)	ICI Cohort2 (N=108)	Non-ICI Cohort (N=36)
<5 cm	18(41.9)	54(50.0)	25(69.4)
Histological Grade — no. (%)			
Poorly differentiated (G3/G4)	14(32.6)	40(37.0)	9(25.0)
Moderately or well differentiated (G1/G2)	13(30.2)	34(31.5)	12(33.3)
NA	16(37.2)	34(31.5)	15(41.7)
PD-L1 expression — no. (%)			
TPS >=1%	4(9.3)	15(13.9)	3(8.3)
TPS<1%	22(51.2)	39(36.1)	17(47.2)
NA	17(39.5)	54(50.0)	16(44.4)
Best response rate — no. (%)			
PR	6(14.0)	18(16.7)	3(8.3)
SD	18(41.9)	62(57.4)	14(38.9)
PD	16(37.1)	24(22.2)	3(8.3)
NA	3(7.0)	4(3.7)	16(44.4)
Clinical benefit — no. (%)			
DCB	13(30.2)	54(50.0)	11(30.6)
NCB	30(69.8)	51(47.2)	10(27.8)
NA	0(0.0)	3(2.8)	15(41.7)
PFS — Median (95%CI) month			
PFS-All	4.16(2.84-5.47)	4.13(2.14-6.13)	6.03(3.87-8.17)
PFS-HCC	10.73(1.62-19.84)	6.63(3.77-9.49)	6.03(3.53-8.54)
PFS-BTC	3.06(1.26-4.88)	3.5(3.00-4.01)	4.93(3.54-6.32)
PFS-CHCC	2.66(2.51-2.83)	NA	NA
OS — Median (95%CI) month			
OS-All	13.53(8.10-19.0)	12.73(9.23-16.24)	10.07(6.96-13.17)
OS-HCC	NR	17.43(8.06-26.81)	8.33(7.79-8.88)
OS -BTC	10.13(6.56-13.71)	12.03(8.78-15.28)	9.79(3.51-41.96)
OS -CHCC	NA	NA	NA

Abbreviations: OS: overall survival, PFS: progression-free survival, CI: confidence interval, PR: partial response, SD: stable disease, PD: progressive disease, DCB: durable clinical benefit, NCB: no clinical benefit, NA: not available ,NR: not reach, NAFLD: Non-alcoholic fatty liver disease, AFLD: alcoholic fatty liver disease

Figure S1

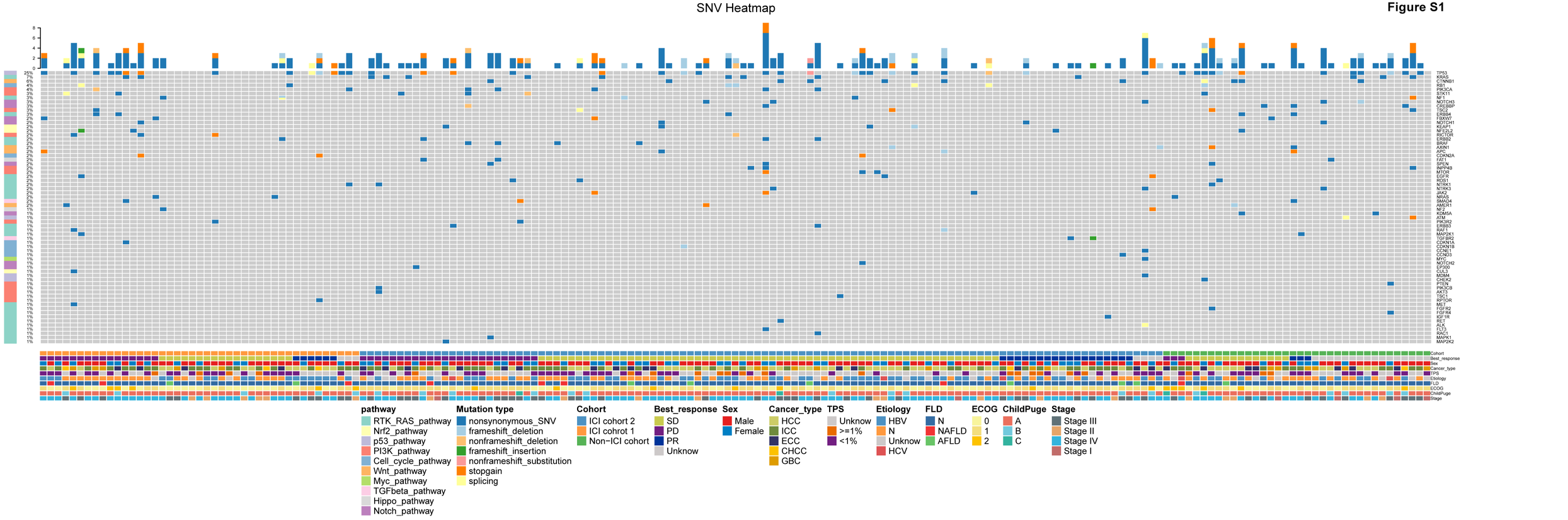

Figure S2

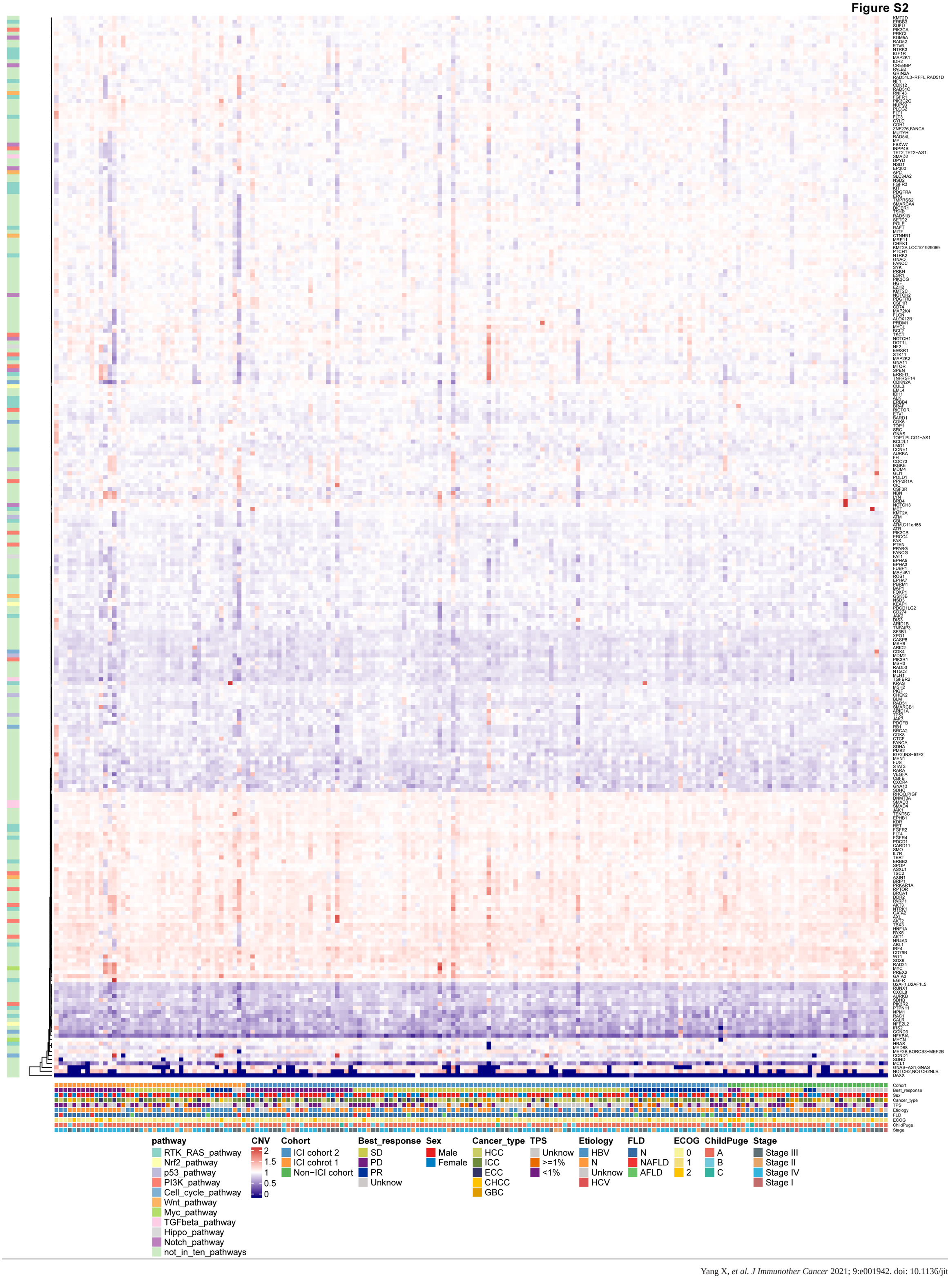
KMT2D
ERBB3
SUFU
PIK3CA
PRKCI
KDM5A
RAD52
ETV6
NTRK3
IGF1R
MAP2K1
IDH2
CREBBP
PALB2
GRIN2A
RAD51L3−RFFL,RAD51D
NF1
CDK12
RAD51C
RNF43
FGFR1
PIK3C2G
NUP93
PLCG2
FLT1
FLT3
CYLD
CDH1
ZNF276,FANCA
MUTYH
RAD54L
MPL
FBXW7
INPP4B
TET2,TET2−AS1
SMAD2
DPYD
NSD1
EP300
APC
SLC34A2
NSD2
FGFR3
KIT
PDGFRA
ERG
TMPRSS2
SMARCA4
DICER1
TSHR
RAD51B
SETD2
POLE
RAF1
MITF
CTNNB1
MRE11
CHEK1
KMT2A,LOC101929089
PTCH1
NTRK2
GNAQ
FANCC
SYK
PRKN
ESR1
PIK3CG
HGF
EZH2
KMT2C
NOTCH2
PDGFRB
CSF1R
CD74
MAP2K4
FLCN
ALOX12B
PRDM1
MYCL
BCL2
TSC1
NOTCH1
DOT1L
NF2
EWSR1
STK11
MAP2K2
GNA11
MTOR
SPEN
ERRFI1
TNFRSF14
CDKN2A
CUL3
EML4
IDH1
ALK
ERBB4
BRAF
RICTOR
ETV1
BARD1
CDK6
TOP1
SRC
GNAS
TOP1,PLCG1−AS1
BCL2L1
LMO1
CCNE1
AURKA
FH
CDC73
IKBKE
MDM4
GLI1
POLD1
PPP2R1A
CIC
CSF3R
NBN
LYN
BRD4
NOTCH3
MET
KMT2A
ATM
CBL
ATM,C11orf65
ATR
PIK3CB
ERCC4
FAS
PTEN
PPARG
FANCG
FAT1
EPHA5
EPHA3
FUBP1
MAP3K1
ROS1
EPHA7
PBRM1
BAP1
FOXP1
GSK3B
NSD3
KEAP1
PDCD1LG2
CD274
JAK2
DIS3
ARID1B
TNFAIP3
SF3B1
XPO1
CASP8
MSH6
ARID2
CDK4
MDM2
PIK3R1
MSH3
RAD50
NT5C2
MLH1
TGFBR2
KRAS
MSH2
PIGF
CHEK2
BLM
RAD51
SMARCB1
ARID1A
TP53
JAK3
PDGFB
RB1
BRCA2
CDK8
CTCF
FANCA
SDHA
PMS2
IGF2,INS−IGF2
MEN1
FUS
STAT3
RARA
VEGFA
CBFB
CXCR4
GNA13
SDHC
RHOQ,PIGF
DNMT3A
SMAD3
SMAD4
JAK1
TENT5C
EPHB1
KDR
RET
FGFR2
FLT4
FGFR4
PDCD1
CARD11
SMO
IL7R
TERT
ERBB2
SPOP
ASXL1
TSC2
AXIN1
BRIP1
PRKAR1A
RPTOR
BRCA1
DDR2
PARP1
AKT3
NTRK1
GATA2
AXL
AKT2
TBX3
HNF1A
PAX5
AKT1
NR4A3
ABL1
IRF4
CD79B
WT1
SOX9
RAD21
MYC
PREX2
GATA3
EGFR
U2AF1,U2AF1L5
RUNX1
CXCL8
AURKB
SDHB
PIK3R2
PTPN11
NPM1
RAC1
CALR
NFE2L2
IRS2
CCND3
NFKBIA
MYCN
HRAS
MYD88
MEF2B,BORCS8−MEF2B
CCND1
SDHD
MCL1
GNAS−AS1,GNAS
NOTCH2,NOTCH2NLR
DAXX
Cohort
Best_response
Sex
Cancer_type
TPS
Etiology
FLD
ECOG
ChildPuge
Stage
pathway
RTK_RAS_pathway
Nrf2_pathway
p53_pathway
PI3K_pathway
Cell_cycle_pathway
Wnt_pathway
Myc_pathway
TGFbeta_pathway
Hippo_pathway
Notch_pathway
not_in_ten_pathways
CNV
2
1.5
1
0.5
0
Cohort
ICI cohort 2
ICI cohrot 1
Non−ICI cohort
Best_response
SD
PD
PR
Unknow
Sex
Male
Female
Cancer_type
HCC
ICC
ECC
CHCC
GBC
TPS
Unknow
>=1%
<1%
Etiology
HBV
N
Unknow
HCV
FLD
N
NAFLD
AFLD
ECOG
0
1
2
ChildPuge
A
B
C
Stage
Stage III
Stage II
Stage IV
Stage I

Figure S3

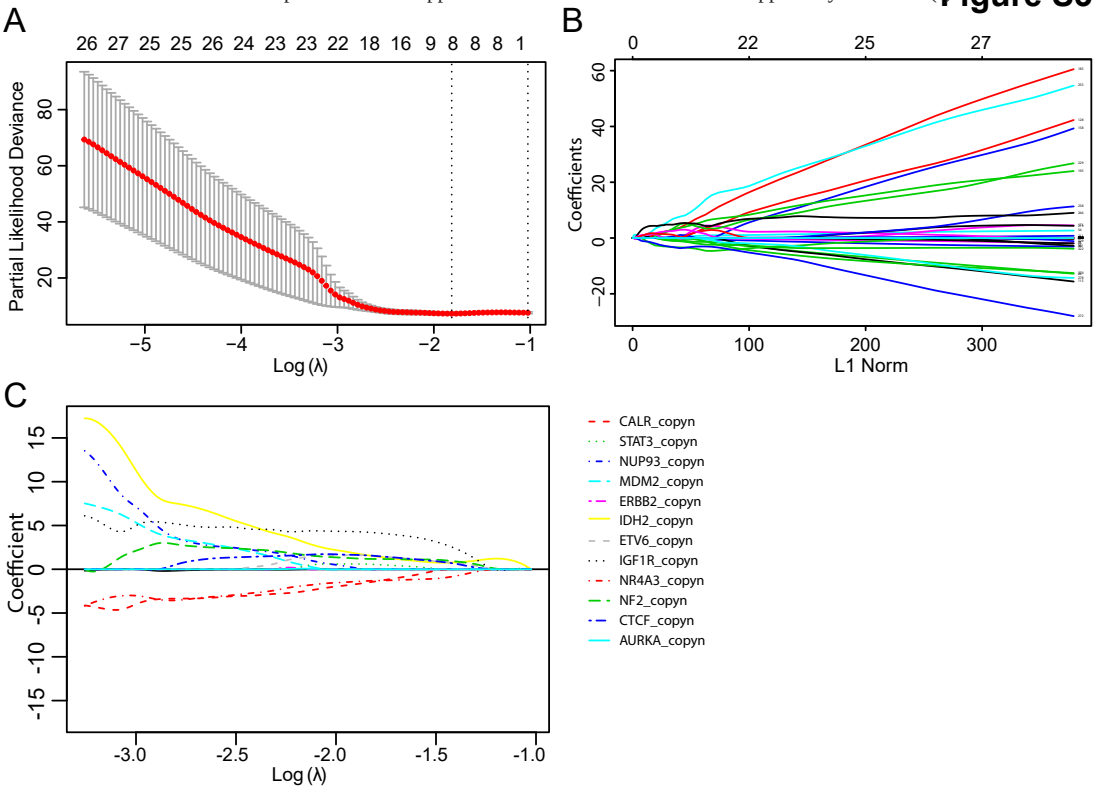
A
26 27 25 25 26 24 23 23 22 18 16 9 8 8 8 1
Partial Likelihood Deviance
Log (λ)
B
0 22 25 27
Coefficients
L1 Norm
C
Coefficient
Log (λ)
CALR_copyn
STAT3_copyn
NUP93_copyn
MDM2_copyn
ERBB2_copyn
IDH2_copyn
ETV6_copyn
IGF1R_copyn
NR4A3_copyn
NF2_copyn
CTCF_copyn
AURKA_copyn

Figure S5

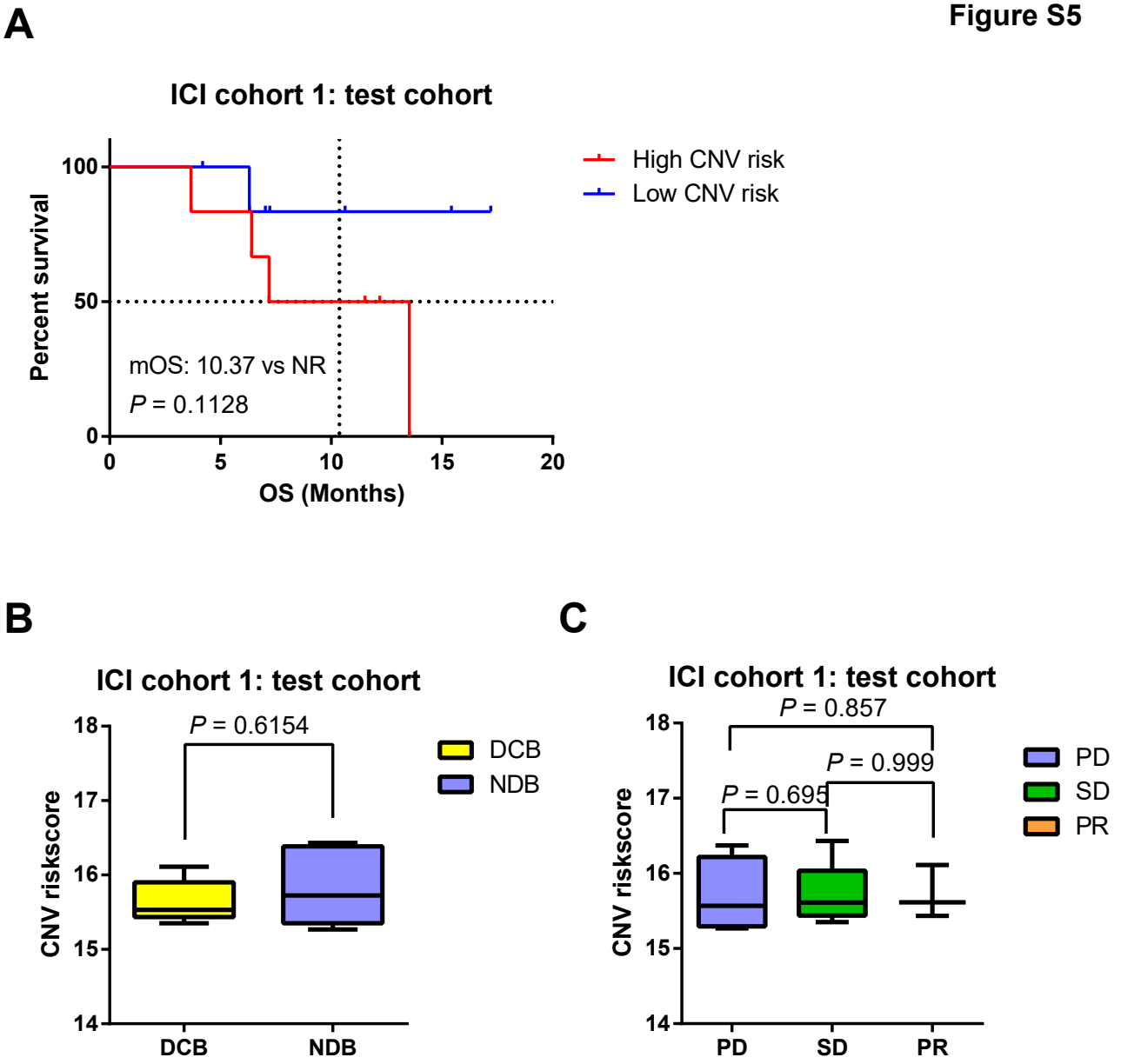
A
ICI cohort 1: test cohort
Percent survival
100
50
0
0
5
10
15
20
OS (Months)
mOS: 10.37 vs NR
P = 0.1128
High CNV risk
Low CNV risk
B
ICI cohort 1: test cohort
CNV riskscore
18
17
16
15
14
P = 0.6154
DCB
NDB
DCB
NDB
C
ICI cohort 1: test cohort
CNV riskscore
18
17
16
15
14
P = 0.857
P = 0.999
P = 0.695
PD
SD
PR
PD
SD
PR

Supplementary Table 2. The correction between CNV risk score with clinicopathological characteristics

Variable	Category	High-risk (N=71)	Low-risk (N=80)	P value (Fisher's exact test)
Sex	Female	28 (39.4)	25 (47.2)	0.310
	Male	43 (60.6)	55 (56.1)	
Age	<60	34 (47.9)	39 (48.8)	1
	>=60	37 (52.1)	41 (51.2)	
Histological Type	BTC	52 (73.2)	39 (48.8)	**0.004**
	CHCC	2 (2.8)	2 (2.6)	
	HCC	17 (23.9)	39 (48.8)	
Histological Grade	Moderately or well differentiated	42 (59.2)	55 (68.8)	0.238
	Poorly differentiated	29 (40.8)	25 (31.3)	
Macrovascular Invasion	N	54 (76.1)	65 (81.3)	0.550
	Y	17 (23.9)	15 (18.8)	
TNM Stage	I-III	30 (42.3)	29 (36.3)	0.505
	IV	41 (57.7)	51 (63.7)	
Tumor burden score	<8	37 (52.1)	57 (71.3)	**0.019**
	>=8	34 (47.9)	23 (28.7)	
Maximum tumor diameter	<5	27 (38.0)	52 (65.0)	**0.001**
	>=5	44 (62.0)	28 (35.0)	

Abbreviations: HCC: hepatocellular carcinoma, BTC: biliary tract cancer, CHCC: combined hepatocellular-cholangiocarcinoma, CNV: copy number variation

Figure S4

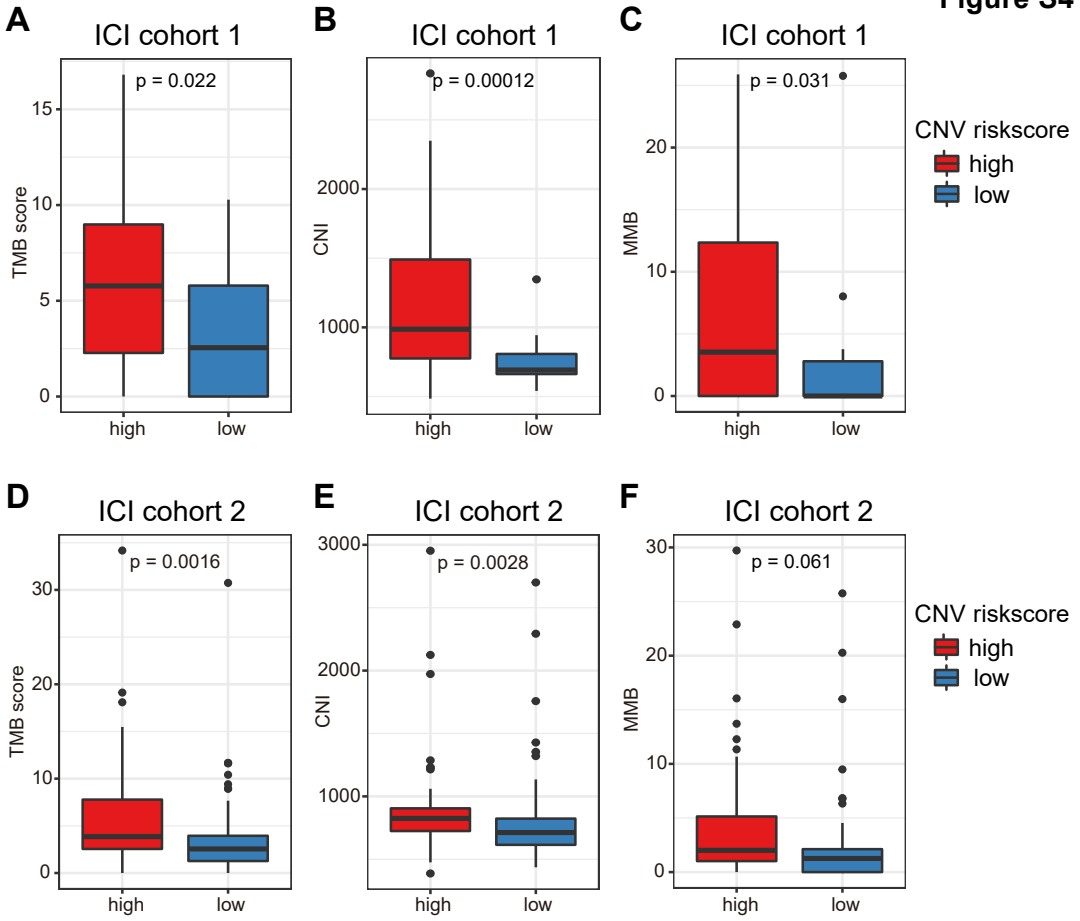
A
ICI cohort 1
p = 0.022
TMB score
high
low
B
ICI cohort 1
p = 0.00012
CNI
high
low
C
ICI cohort 1
p = 0.031
MMB
high
low
CNV riskscore
high
low
D
ICI cohort 2
p = 0.0016
TMB score
high
low
E
ICI cohort 2
p = 0.0028
CNI
high
low
F
ICI cohort 2
p = 0.061
MMB
high
low
CNV riskscore
high
low

Figure R1

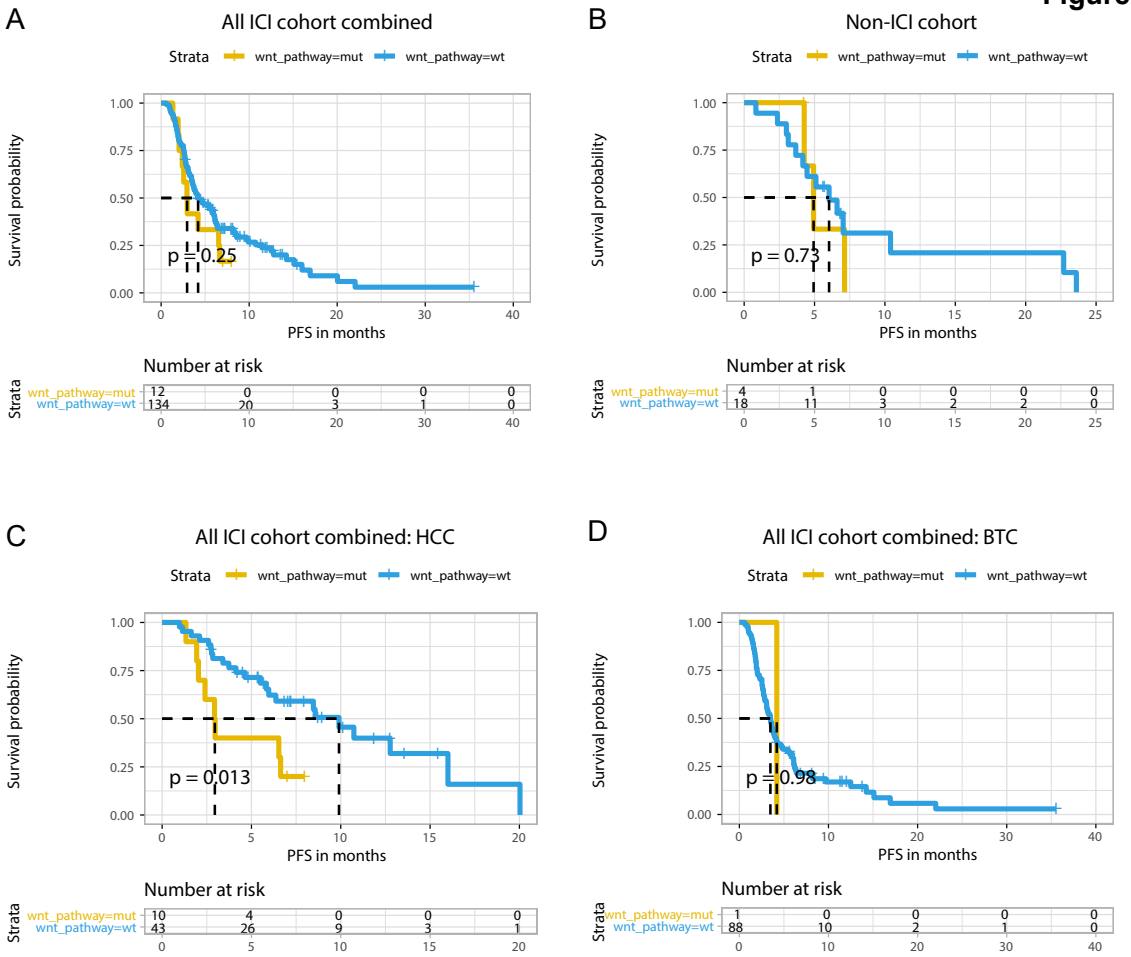
A
All ICI cohort combined
Strata wnt_pathway=mut wnt_pathway=wt
Survival probability
p = 0.25
PFS in months
Number at risk
wnt_pathway=mut 12 0 0 0 0
wnt_pathway=wt 134 20 3 1 0
B
Non-ICI cohort
p = 0.73
wnt_pathway=mut 4 1 0 0 0 0
wnt_pathway=wt 18 11 3 2 2 0
C
All ICI cohort combined: HCC
p = 0.013
wnt_pathway=mut 10 4 0 0 0
wnt_pathway=wt 43 26 9 3 1
D
All ICI cohort combined: BTC
p = 0.98
wnt_pathway=mut 1 0 0 0 0
wnt_pathway=wt 88 10 2 1 0

Figure R2

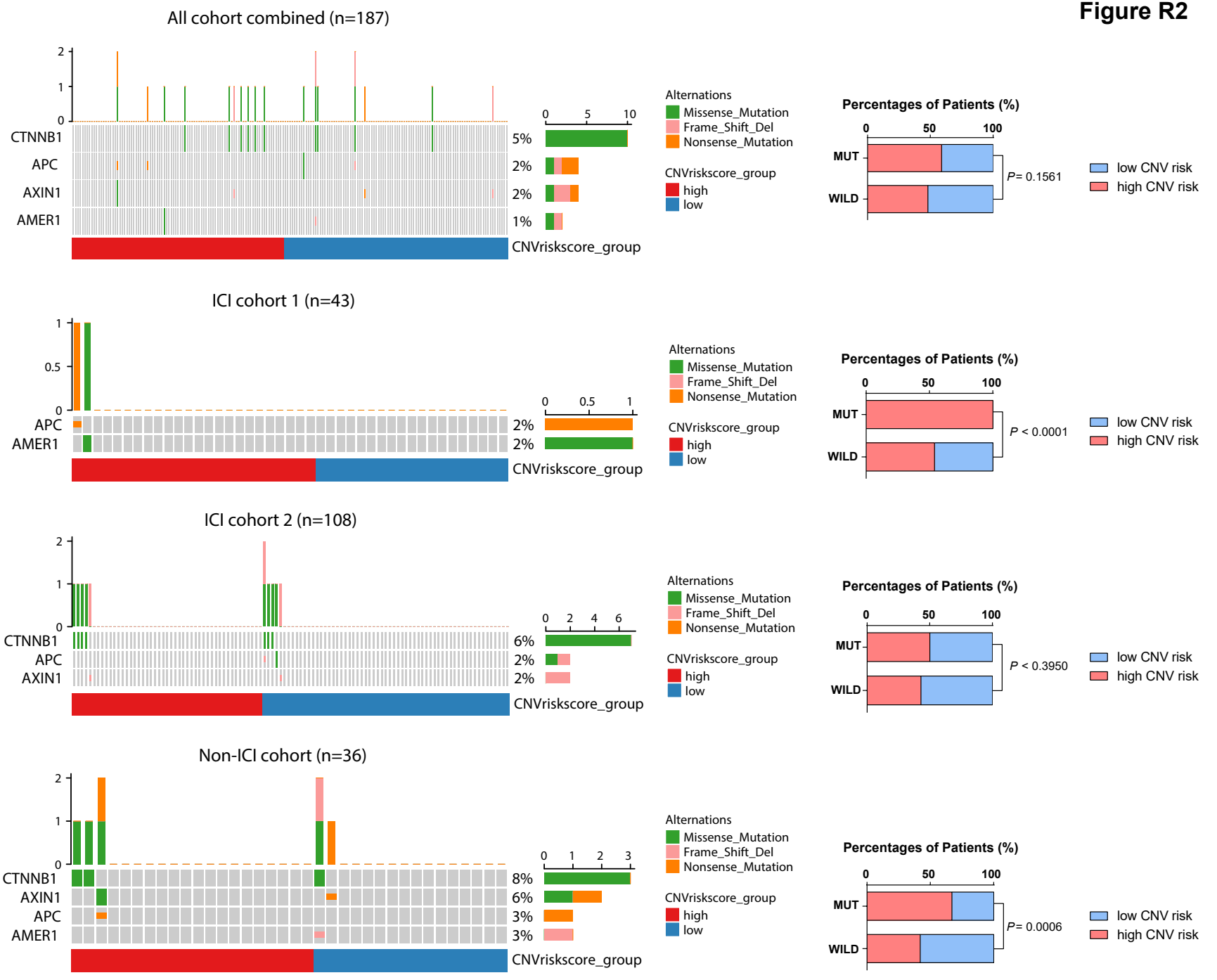
All cohort combined (n=187)
CTNNB1
APC
AXIN1
AMER1
5%
2%
2%
1%
CNVriskscore_group
Alternations
Missense_Mutation
Frame_Shift_Del
Nonsense_Mutation
CNVriskscore_group
high
low
Percentages of Patients (%)
MUT
WILD
P= 0.1561
low CNV risk
high CNV risk
ICI cohort 1 (n=43)
APC
AMER1
2%
2%
P < 0.0001
ICI cohort 2 (n=108)
CTNNB1
APC
AXIN1
6%
2%
2%
P < 0.3950
Non-ICI cohort (n=36)
CTNNB1
AXIN1
APC
AMER1
8%
6%
3%
3%
P= 0.0006

北京協和醫院
PEKING UNION MEDICAL COLLEGE HOSPITAL

PROTOCOL NUMBER: [JS-1864]

PROTOCOL TITLE: [Lenvatinib Combined Pembrolizumab in Advanced Hepatobiliary Tumors]

IRB APPROVAL DATE: **[2019-01-22]**

IRB APPROVAL TYPE: **Standard Review**

Dear Dr. Haitao Zhao

The Institutional Review Board (IRB) of Peking Union Medical College Hospital (PUMCH)has reviewed the above-named protocol and has determined that 1) the applicant(s) are qualified to conduct the proposed study; 2) the design of the study is rationale and scientifically sound; 3) human subject protection is adequate and 4) the informed consent is acceptable. The IRB thus approve the protocol.

This approval is valid for one year from the date of IRB review and will no longer be in effect on the date listed above as the IRB expiration date. A Continuing Review application must be approved before the expiration date to avoid cessation of all research activities.

It is the responsibility of all investigators and research staff to promptly report to the IRB any adverse and unexpected events, protocol deviation or violations and unanticipated problems which may impose risks on subjects.

Signature of Chairman of IRB member: Zhaohui Zhu

PUMCH Institutional Review Board

北京協和醫院
PEKING UNION MEDICAL COLLEGE HOSPITAL

PROTOCOL NUMBER: **[JS-1391]**

PROTOCOL TITLE: [Real-world Study for Patients With Advanced Hepatobiliary Tumors]

IRB APPROVAL DATE: **[2017-07-25]**

IRB APPROVAL TYPE: **Standard Review**

Dear Dr. Haitao Zhao

The Institutional Review Board (IRB) of Peking Union Medical College Hospital (PUMCH)has reviewed the above-named protocol and has determined that 1) the applicant(s) are qualified to conduct the proposed study; 2) the design of the study is rationale and scientifically sound; 3) human subject protection is adequate and 4) the informed consent is acceptable. The IRB thus approve the protocol.

This approval is valid for one year from the date of IRB review and will no longer be in effect on the date listed above as the IRB expiration date. A Continuing Review application must be approved before the expiration date to avoid cessation of all research activities.

It is the responsibility of all investigators and research staff to promptly report to the IRB any adverse and unexpected events, protocol deviation or violations and unanticipated problems which may impose risks on subjects.

Signature of Chairman of IRB member: Zhaohui Zhu

PUMCH Institutional Review Board